

Oak Ridge National Laboratory Critical Experiment Design Phase 1 Report for Integral Request 441



J. B. Clarity
D. E. Mueller
W. J. Marshall
R. M. Westfall

07/14/2017

Approved for public release.
Distribution is unlimited.

DOCUMENT AVAILABILITY

Reports produced after January 1, 1996, are generally available free via US Department of Energy (DOE) SciTech Connect.

Website <http://www.osti.gov/scitech/>

Reports produced before January 1, 1996, may be purchased by members of the public from the following source:

National Technical Information Service
5285 Port Royal Road
Springfield, VA 22161
Telephone 703-605-6000 (1-800-553-6847)
TDD 703-487-4639
Fax 703-605-6900
E-mail info@ntis.gov
Website <http://classic.ntis.gov/>

Reports are available to DOE employees, DOE contractors, Energy Technology Data Exchange representatives, and International Nuclear Information System representatives from the following source:

Office of Scientific and Technical Information
PO Box 62
Oak Ridge, TN 37831
Telephone 865-576-8401
Fax 865-576-5728
E-mail reports@osti.gov
Website <http://www.osti.gov/contact.html>

This report was prepared as an account of work sponsored by an agency of the United States Government. Neither the United States Government nor any agency thereof, nor any of their employees, makes any warranty, express or implied, or assumes any legal liability or responsibility for the accuracy, completeness, or usefulness of any information, apparatus, product, or process disclosed, or represents that its use would not infringe privately owned rights. Reference herein to any specific commercial product, process, or service by trade name, trademark, manufacturer, or otherwise, does not necessarily constitute or imply its endorsement, recommendation, or favoring by the United States Government or any agency thereof. The views and opinions of authors expressed herein do not necessarily state or reflect those of the United States Government or any agency thereof.

Reactor and Nuclear Systems Division

Critical Experiment Design Phase 1 for Integral Experiment Request 441

Justin B. Clarity
William (B. J.) Marshall
Don E. Mueller
Robert M. Westfall

Date Published: 9/30/2017

Prepared by
OAK RIDGE NATIONAL LABORATORY
Oak Ridge, TN 37831-6283
managed by
UT-BATTELLE, LLC
for the
US DEPARTMENT OF ENERGY
under contract DE-AC05-00OR22725

CONTENTS

CONTENTS	iii
ABSTRACT	1
1. Introduction	2
2. Experimental Description	2
3. Anticipated Critical Configurations	4
3.1 Dysprosium	8
3.2 Hafnium	12
3.3 Silver	16
3.4 Tantalum	20
3.5 Indium	24
3.6 Cobalt	28
3.7 Tungsten	32
3.8 Manganese	36
3.9 Antimony	40
4. Conclusions and CED-2 Actions	44
5. References	46

ABSTRACT

This report documents the analytical methods used in the first phase of critical experiment design (CED-1) conducted as part of integral experiment request (IER) 441. The purpose of IER-441 is to develop a capability to test the epithermal/intermediate cross sections of materials at the Sandia National Laboratories (SNL) critical experiment facility using low enriched uranium oxide fuel. This effort determined that the capability can be achieved using a varying number of test samples placed in a central test region of a hexagonally pitched lattice driven with a more moderated exterior region. In general, the results show that it is possible to develop sufficient worth to measure any nuclear data deficiencies, as well as the ability to shift the neutron spectrum for dysprosium, hafnium, silver, tantalum, indium, cobalt, tungsten, and antimony. There is marginal capability to test manganese due to its relatively low worth at higher boron concentrations. At this stage, there is interest in identifying the material or materials of greatest interest to the nuclear data community so that this project can proceed to CED-2 with a clear goal.

1. INTRODUCTION

Nuclear criticality safety (NCS) evaluations commonly take credit for neutron-absorbing materials. The normal practice for validating the calculational process to develop safety limits and margins of safety is to compare the safety case models with calculations of various critical experiments of a similar composition. Because there is a lack of critical experiments with various relevant neutron-absorbing materials mixed with fissile material, a new approach is being developed. This new approach uses small amounts of these credited materials in a critical assembly and assesses their worth and neutron energy spectral characteristics using absorption reaction rates. This approach is proposed as a new method for nuclear data validation. The assessment will involve measured central reactivity worth in a critical or near-critical assembly and subsequent comparison with calculated values from Monte Carlo computer analyses.

This report documents the critical experiment design process phase 1 (CED-1) assessment of integral experiment request (IER) 441. The scope of IER-441 is to develop an ability to test epithermal/intermediate energy cross sections for materials using the 7uPCX critical experiment facility. This report uses the lattice proposed as part of the *Safety Technology for Environmental Management – Neutron Spectra Experiments for Underpinning Safety* (STEM -NEXUS) report [1]. Because no specific test material is identified for this project, several materials are investigated here with the expectation that nuclear data professionals can identify materials of interest to the Nuclear Criticality Safety Program.

Section 2 of this report discusses the overall experimental layout and conceptual description. Section 3 describes the possible critical configurations that could be attained, and it provides a discussion of the impact they have on the neutron energy distribution contributing to the worth of the test material. Section 4 presents the conclusions of this effort and details the action items to be addressed for CED-2. Section 5 includes references.

2. EXPERIMENTAL DESCRIPTION

The proposed IER-441 experiments will be carried out using (1) the 7uPCX fuel at Sandia National Laboratories (SNL) and (2) the new tight pitch hexagonal grid plates. The 7uPCX fuel is 6.90 wt% enriched UO_2 fuel that has been used in previous critical experiments [2,3,4]. The nominal outside diameter of the fuel pellets is 0.207 inches (0.52578 cm), and the nominal outside diameter of the cladding is 0.250 inches (0.635 cm) with a 0.014-inch (0.03556 cm) wall thickness. The critical facility containing the 7uPCX fuel can approach critical based on the number of fuel rods or the height of the moderating and reflecting water. The expected critical configurations are similar to the critical experiment configurations present in LEU-COMP-THERM-080, -096, and -097, except that the lattice has been changed to a tight-pitched hexagonal configuration. An overview of the experimental setup from LEU-COMP-THERM-097 is provided in Fig. 1, which shows the locations of the fuel rods, detectors, grid plates, ^{252}Cf source, and water level monitors. The experimental setup for the IER-441 effort would be the same as that shown except for the grid plate and a central aluminum block designed to exclude the moderator from the region immediately surrounding the test materials.

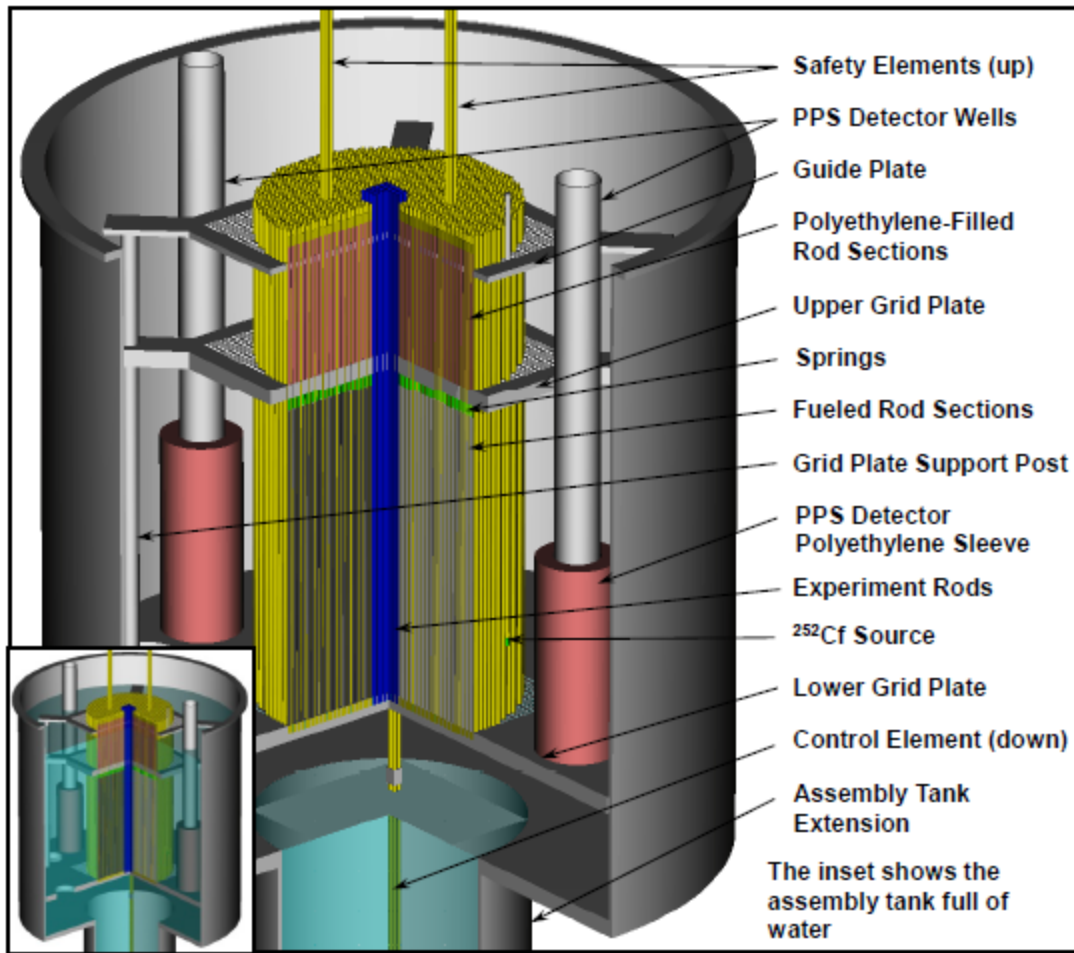


Fig. 1. Experimental apparatus from LEU-COMP-THERM-097 [46].

The proposed lattice is arranged with a three-region hexagonal design. The innermost region, which is the test region, is an aluminum block with 37 holes arranged in 4 rings. The inner aluminum block will hold the test material samples. The test material pins would have the same diameter as the 7uPCX fuel rods to facilitate fuel pin replacement experiments operating in a more thermal spectrum if that becomes desirable. Additional borated aluminum blocks can be fabricated with variable concentrations of boron (0, 1, 2, and 5 wt%). Including other blocks that have thermal neutron absorbers will provide the ability to shift the spectrum of neutrons contributing to the reaction rate in the test material to higher energies. Borated aluminum is commercially available [5]. The second region of the lattice is the close-packed region that includes fuel rods in every location. The close-packed region is designed to have the highest fuel-to-moderator ratio possible while maintaining criticality with the 7uPCX fuel (pitch = 0.80010 cm). The close-packed region of the lattice requires 510 7uPCX fuel rods and occupies rings 5 through 14. The third region of the configuration is the driver region, which is arranged with the same center-to-center pitch as the close-packed region, except every other rod in every other ring has been removed to increase moderation and drive system reactivity. The driver region is far enough away from the test region to allow for a harder flux spectrum near the test sample. The driver region uses 1,145 rods and occupies rings 15–27 (the remainder of the lattice). Fig. 2 depicts the proposed STEM-NEXUS lattice.

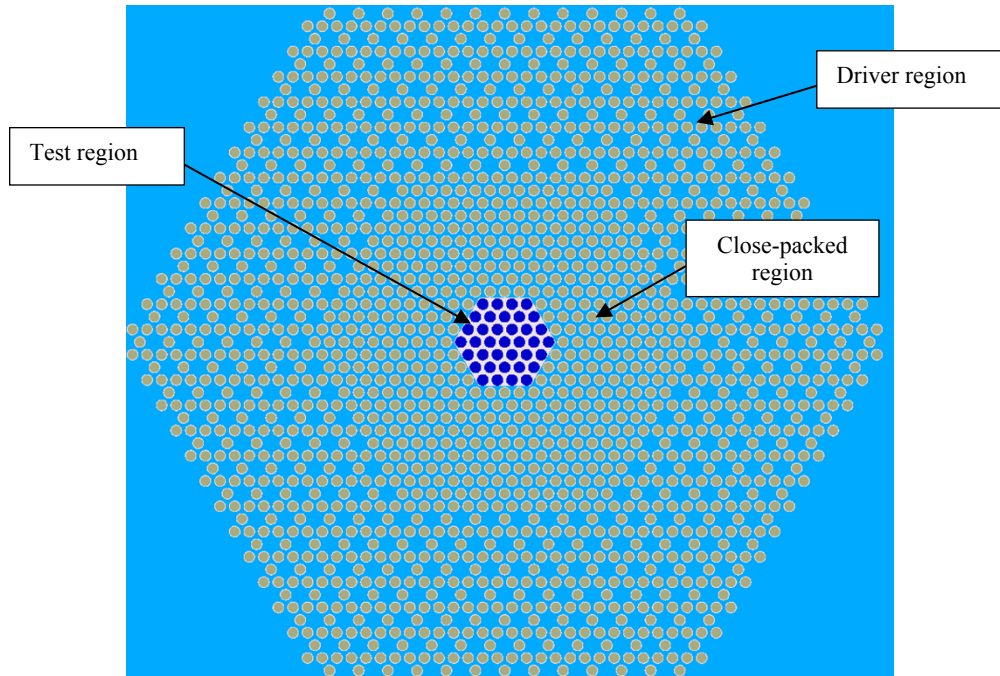


Fig. 2. STEM-NEXUS lattice as proposed in Westfall [1]; additional water around lattice edge not shown.

3. ANTICIPATED CRITICAL CONFIGURATIONS

Because of ambiguity in the test material specification, it was decided that the scope of CED-1 should focus on defining what information could be extracted from the proposed lattice for a variety of materials so that nuclear data experts could then provide feedback on the need for and usefulness of the information that can be provided. The process followed for each material investigated was as follows:

1. Calculate the k_{eff} for the configuration with an empty central block.
2. Calculate the worth (Δk_{eff}) with the central aluminum block locations filled with a varying number of rods of the test material in the central test region.
3. Repeat the process with the aluminum block with variable amounts of boron in the central block.
4. Compare the reaction rates for the materials in the test region to determine whether the portion of the cross section contributing to the worth of the test material can be shifted.

Several elements were considered that (1) occur naturally in the solid phase, (2) appear to have some value to nuclear operations, and (3) do not have an exorbitant price (e.g., platinum was excluded). The list of materials examined during this effort is included below in Table 1. This is not an exhaustive list of elements; other materials may be examined if a specific need is identified.

Table 1. List of elements examined during IER-441

Dysprosium (Dy)	Hafnium (Hf)	Silver (Ag)	Tantalum (Ta)
Indium (In)	Cobalt (Co)	Tungsten (W)	Manganese (Mn)
Antimony (Sb)	Molybdenum (Mo)	Titanium (Ti)	Iron (Fe)
Vanadium (V)	Copper (Cu)	Niobium (Nb)	Calcium (Ca)
Strontium (Sr)	Chromium (Cr)	Tin (Sn)	

The purpose of IER-441 is to develop an experiment to provide insight into the quality of evaluated cross section data of materials in the epithermal-to-intermediate range using the SNL critical facility. To that end, a method must be developed to change the worth of the test material by varying the energy regions being tested. Preliminary calculations showed that this can be accomplished in two ways. The first mechanism takes advantage of the ability to saturate the thermal reaction rate using the self-shielding effect by varying the amount of test material. The second method is to decrease the thermal worth of the test material by introducing a predominantly thermal absorber (boron) while hoping to preserve the worth of the material in the higher energy regions. For the purposes of IER-441, the saturation effect is examined by varying the number of pins in the test region and then examining the effect on the reaction rate and worth of the test material. The spectrum in the region immediately surrounding the test material was adjusted by including a small amount of natural boron in the aluminum block holding the test material. Boron concentrations used for this report are 1, 2, and 5 wt%. While the saturation and thermal competition effects are treated separately in this report, they would be used in conjunction with each other in practice. All calculations for this effort were performed with the SCALE 6.2.1 version of KENO-VI using the continuous energy version of the ENDF/B-VII.1 cross section library. The reaction rate results presented are formatted in the default 252-group structure used by SCALE for criticality calculations. The 252-group structure is sufficient for showing the spectral variation of the absorption reaction rates for this purpose. All material specifications are taken from the SCALE standard composition library as their pure metallic form.

The first step in evaluating the ability to test individual materials was to determine their worths in the possible experimental configurations. The parameter used to control criticality for the experiment will be the number of rods in the array. The worths (Δk_{eff}) are expected to be insensitive (within reason) to the number of fuel rods in the array. Therefore, the worths are calculated by subtracting the k_{eff} of the fully flooded rod array with an empty test region full of the test material from the k_{eff} of a fully flooded array with an empty test region. The maximum worth in the unborated systems was calculated by placing solid pins that are equal in diameter to the fuel pins into each of the 37 central locations. Discussions with researcher Gary Harms of SNL indicate that it is possible to measure critical or near-critical configurations with an uncertainty of approximately $0.00100 \Delta k_{\text{eff}}$ for uncorrelated experiments, and it is also possible to measure critical or near-critical configurations correlated with an uncertainty of $0.00040 \Delta k_{\text{eff}}$. It is important to have enough worth in the test material that any mispredictions due to cross section errors be distinguishable from the experimental uncertainty. The lowest worth evaluated for the next highest concentration of boron in the central region is $\sim 0.00200 \Delta k_{\text{eff}}$, which is five times the correlated experimental uncertainty. The objective is to accurately measure configurations with less than the full 37-pin test region so that trends of the bias versus the total worth of the material can be constructed. Results of the worth calculations are presented in Table 2. Worth calculations were not performed for any element that had a worth of less than $0.00200 \Delta k_{\text{eff}}$ with the previous test region boron concentration.

Table 2. Worths of material examined in a test region of various boron concentrations ($\sigma_{\text{worth}} < 0.00030$) Δk_{eff}

Element	Unborated 37-pin worth	1 wt% boron 37-pin worth	2 wt% boron 37-pin worth	5 wt% boron 37-pin worth
Dy	0.03112	0.02077	0.01677	0.01272
Hf	0.03066	0.02021	0.01619	0.01162
Ag	0.02886	0.01825	0.01501	0.01094
Ta	0.02840	0.01951	0.01617	0.01252
In	0.02664	0.01663	0.01312	0.00877
Co	0.02019	0.01043	0.00725	0.00379
W	0.02032	0.01221	0.00953	0.00581
Mn	0.01185	0.00495	0.00284	0.00101
Sb	0.01070	0.00632	0.00491	0.00431
Mo	0.00586	0.00274	0.00175	NC
Ti	0.00533	0.00094	NC ^a	NC
V	0.00453	0.00015	NC	NC
Cu	0.00437	0.00031	NC	NC
Cr	0.00312	0.00030	NC	NC
Nb	0.00275	0.00092	NC	NC
Fe	0.00220	-0.00065	NC	NC
Sr	0.00130	NC	NC	NC
Sn	0.00093	NC	NC	NC
Ca	-0.00015	NC	NC	NC
Al	-0.00035	NC	NC	NC
Ce	-0.00075	NC	NC	NC
Mg	-0.00146	NC	NC	NC
Pb	-0.00156	NC	NC	NC
Bi	-0.00157	NC	NC	NC

^a NC= not calculated

After the materials are screened to determine if they had sufficient worth to be measured in the STEM-NEXUS lattice, it is necessary to determine if the desired spectral shift is occurring. The materials were examined based on the energy-dependent plots of the absorption reaction rates. Materials selected for further investigation were Dy, Hf, Ag, Ta, In, Co, W, Mn, and Sb due to their reasonably high worth across multiple central block boron concentrations. Each of these elements is discussed further in the following subsections. Gd and Er clearly bear further investigation, but they would not be used in their pure forms. The objective is to demonstrate that the concept can be used for a range of absorber materials.

Reaction rate data were calculated for configurations with unborated test regions with 7, 15, 27, and 37 pins of test material in the test region. The data were also calculated for configurations with 37 pins in test regions with 1, 2, and 5 wt% natural boron. The 7-, 15-, and 27-pin test regions are shown in Fig. 3. Reaction rates are also binned into 5 energy regions: <1 eV, 1 eV–100 eV, 100 eV–1 keV, 1 keV–1 MeV, and >1 MeV. Binning the reactions rates allows for a more quantitative view of how the absorption rate is shifted as a result of adding rods and boron. This is based on a combination of (1) the worth of the material and (2) the ability of the increased number of rods and increased boron concentration of the test region to shift the energy range of the absorption reaction rate. Materials which show high worth and

substantial ability to shift the spectrum of the absorption reaction rate are qualitatively noted as *good* candidate materials, while materials with lower but still easily measurable worths and smaller absorption reaction rate shifts are termed *moderately good*. Materials that have worths high enough to be measured in three or more of the test regions and that show minimal ability to shift the reaction rate spectrum are termed *fair*, and materials that do not show sufficient worth to be measured in more than two of the test regions are termed *poor*.

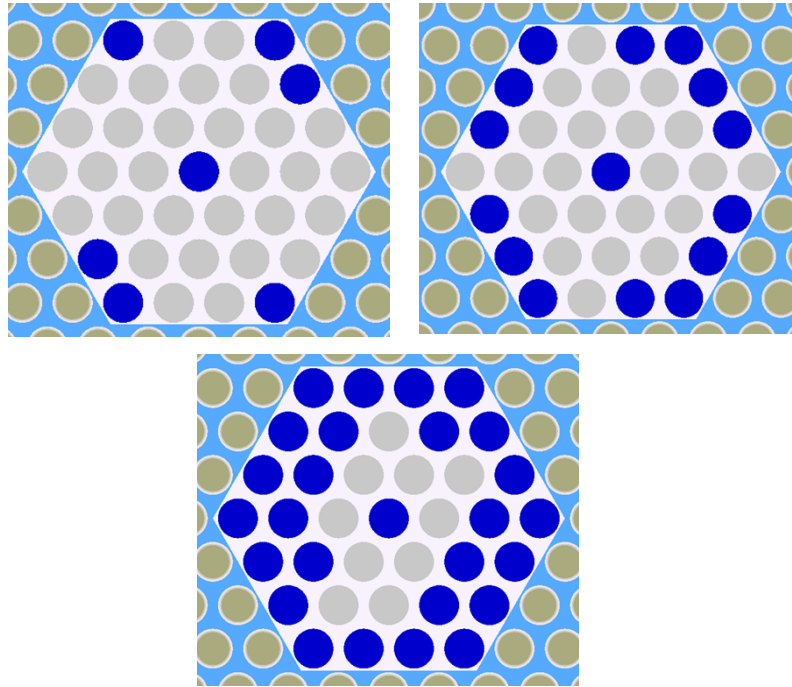


Fig. 3. Test region loaded with 7 (upper left) 15 (upper right) and 27 (lower) test samples.

3.1 DYSPROSIUM

Dysprosium (Dy) is a strong absorber used as a control material in nuclear applications. The isotopic composition of Dy is 19 wt% ^{161}Dy , 25 wt% ^{162}Dy , 25 wt% ^{163}Dy , and 29 wt% ^{164}Dy . A plot of the absorption cross section for these isotopes is included in Fig. 4. The absorption reaction rate for Dy is plotted as a function of energy in Fig. 5 for an unborated test region that includes 7, 15, 27, and 37 test samples. The energy-dependent absorption reaction rate is shown in Fig. 6 for a test region with 37 test samples and boron concentrations of 0, 1, 2, and 5 wt%. Table 3 shows the few-group absorption reaction rates as a percentage of the total absorptions for each of the rod configurations. Fig. 5 shows a strong tendency for the Dy absorption rate to saturate at thermal energies because the reaction rate increases from 7 to 15 samples, but it does not increase with additional samples thereafter. However, the reaction rate increases with additional samples for energies above 10 eV. Fig. 6 shows that the increase in the boron concentration of the central block leads to a significant reduction in the thermal reaction rate, but the reaction rate above the thermal range remains essentially unchanged. Table 3 quantitatively shows that the combination of the number of rods and the boron concentration of the test region block can provide good variability in the fraction of reaction occurring in the various energy regions. Based on these results, it appears that Dy would be a good test material candidate if data about this material are desired.

Table 3. Few group reaction rates for Dy experimental configurations

Number of rods	Boron loading (wt%)	$E < 1 \text{ eV}$ (%)	$1 \text{ eV} < E < 100 \text{ eV}$ (%)	$100 \text{ eV} < E < 1 \text{ keV}$ (%)	$1 \text{ keV} < E < 1 \text{ MeV}$ (%)	$E > 1 \text{ MeV}$ (%)
7	0	18.19	43.81	18.04	18.30	1.66
15	0	19.36	40.70	17.81	20.28	1.85
27	0	20.49	37.63	16.81	22.92	2.15
37	0	21.20	35.47	16.19	24.78	2.36
37	1	12.13	38.79	18.62	27.85	2.61
37	2	8.96	39.24	19.59	29.46	2.76
37	5	5.32	38.72	20.90	32.08	2.99

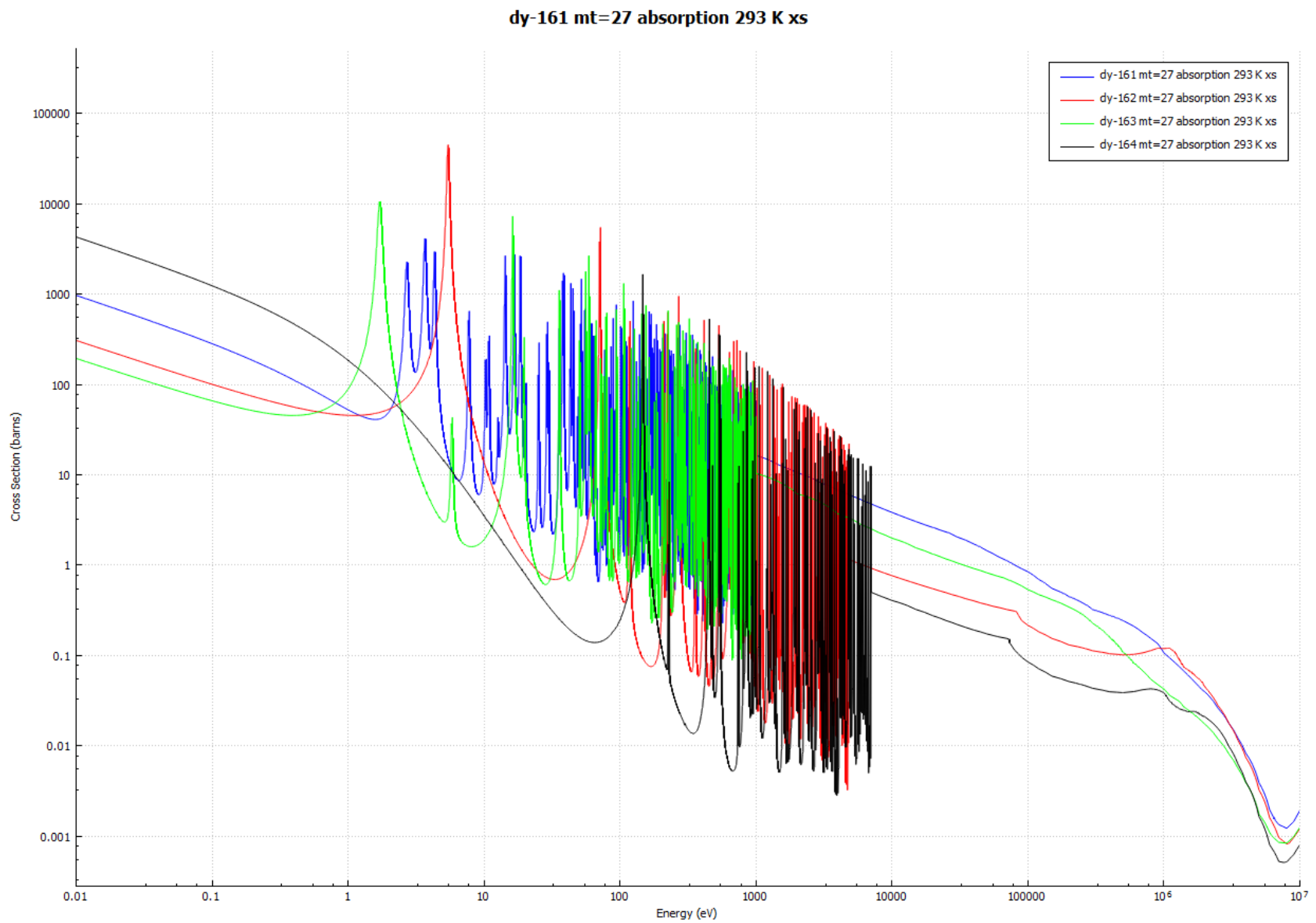


Fig. 4. Energy-dependent absorption cross section for major (>5 wt%) Dy isotopes.

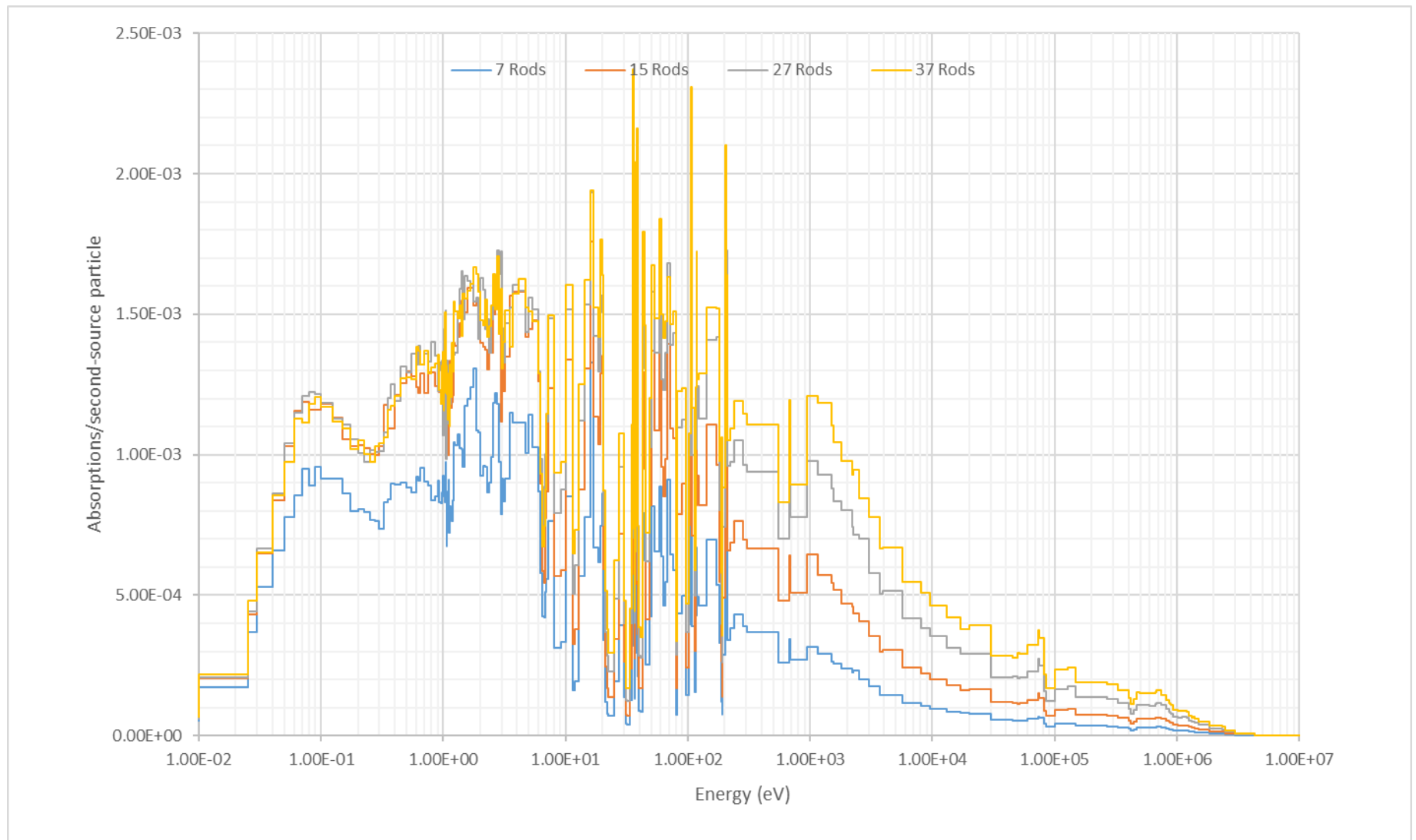


Fig. 5. Energy-dependent reaction rate for a variable number of Dy rods.

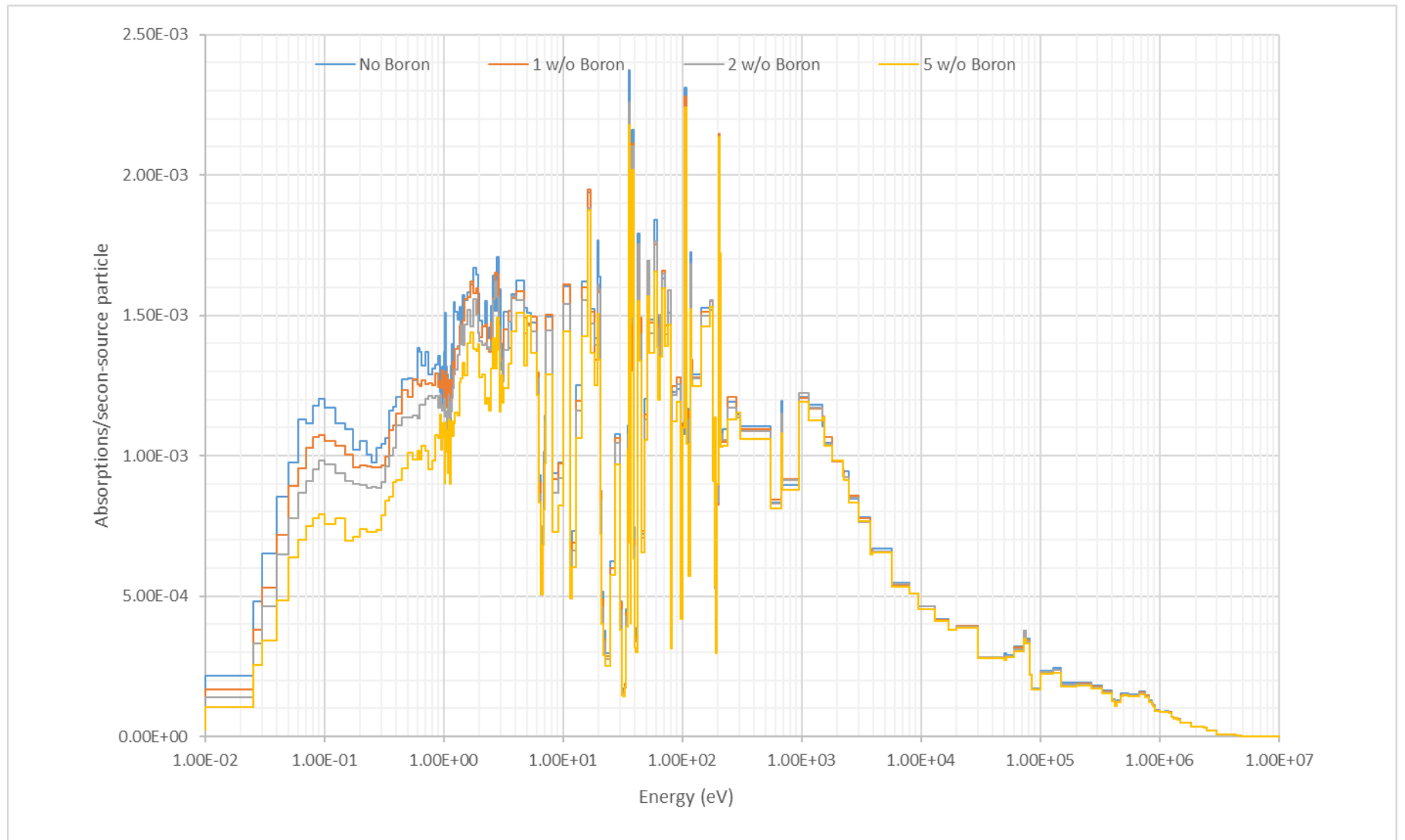


Fig. 6. Energy-dependent reaction rate for 37 Dy rods in a central aluminum block with a variable amount of boron.

3.2 HAFNIUM

Hafnium (Hf) is a strong absorber used in nuclear applications as a control material. This isotopic composition of natural hafnium is 5.2 wt% ^{176}Hf , 18.6 wt% ^{177}Hf , 27.3 wt% ^{178}Hf , 13.6 wt% ^{179}Hf , and 39.0 wt% ^{180}Hf . A plot of the absorption cross section for these isotopes is included in Fig. 7. The absorption reaction rate for Hf is plotted in Fig. 8 as a function of energy for an unborated test region including 7, 15, 27, and 37 test samples. Fig. 9 shows the energy dependent absorption reaction rate for an aluminum test region with 37 test samples and boron concentrations of 0, 1, 2, and 5 wt%. Table 4 shows the few-group absorption reaction rates as a percentage of the total absorptions for each of the rod configurations. Fig. 8 shows a strong tendency for the Hf absorption rate to saturate at thermal energies because the reaction rate increases from 7 to 15 samples, but it does not increase thereafter with additional samples. However, there is an increase in the reaction rate with additional samples for energies above 10 eV. Fig. 9 shows that the increase in the boron concentration of the central block does not lead to a significant reduction in the thermal reaction rate, but the reaction rate above the thermal range remains essentially unchanged. Based on these results, it appears that Hf would be a good test material candidate if data about this material are desired.

Table 4. Few-group reaction rates for Hf experimental configurations

Number of rods	Boron loading (wt%)	$E < 1 \text{ eV}$ (%)	$1 \text{ eV} < E < 100 \text{ eV}$ (%)	$100 \text{ eV} < E < 1 \text{ keV}$ (%)	$1 \text{ keV} < E < 1 \text{ MeV}$ (%)	$E > 1 \text{ MeV}$ (%)
7	0	36.93	41.73	12.65	8.34	0.35
15	0	32.69	40.88	14.77	11.20	0.46
27	0	28.33	38.63	16.94	15.46	0.64
37	0	25.72	36.81	17.95	18.74	0.78
37	1	23.55	37.56	18.67	19.41	0.81
37	2	21.77	38.05	19.34	20.01	0.84
37	5	18.19	37.99	20.61	22.28	0.93

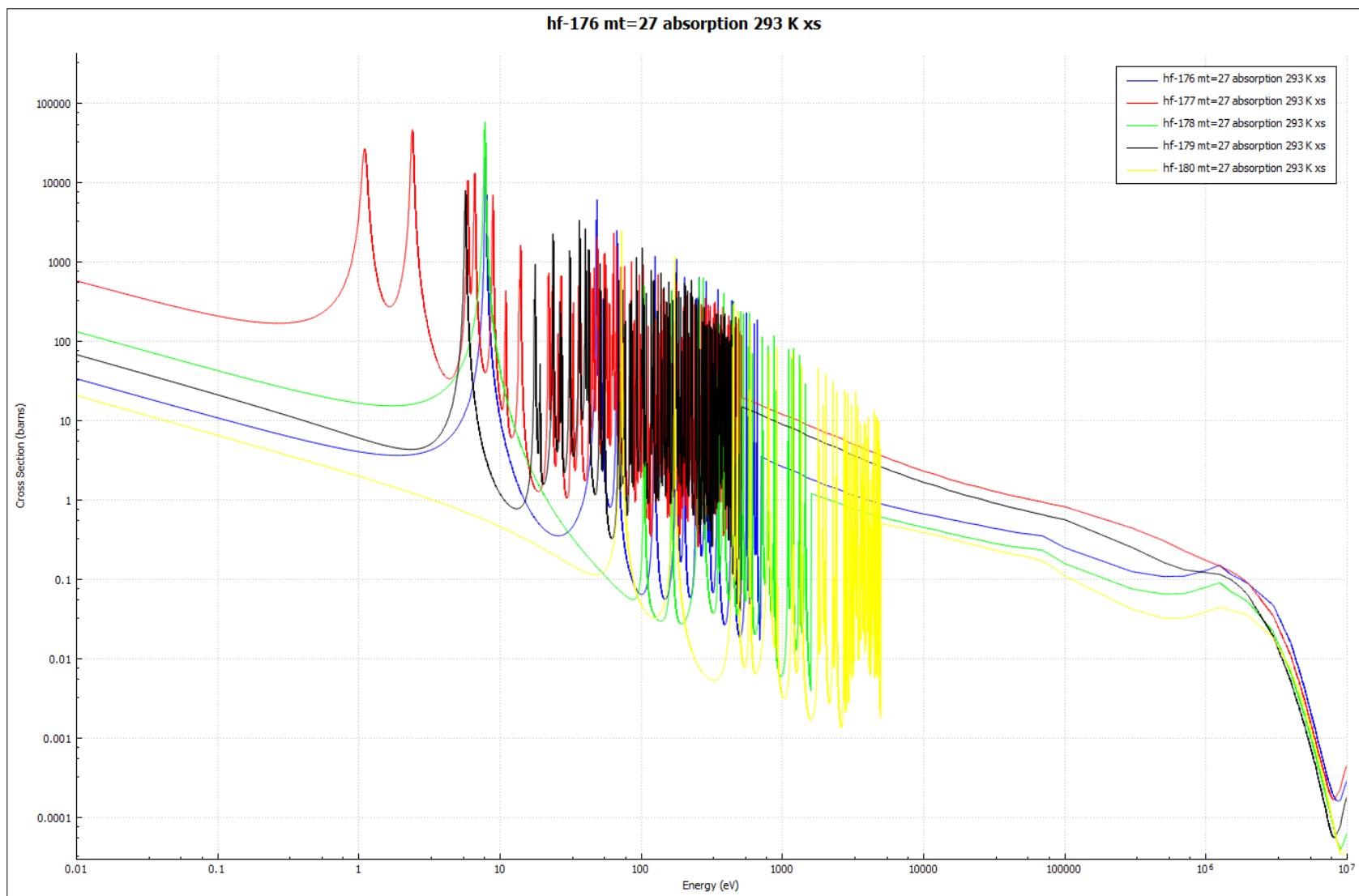


Fig. 7. Energy-dependent absorption cross section for major (>5 wt%) Hf isotopes.

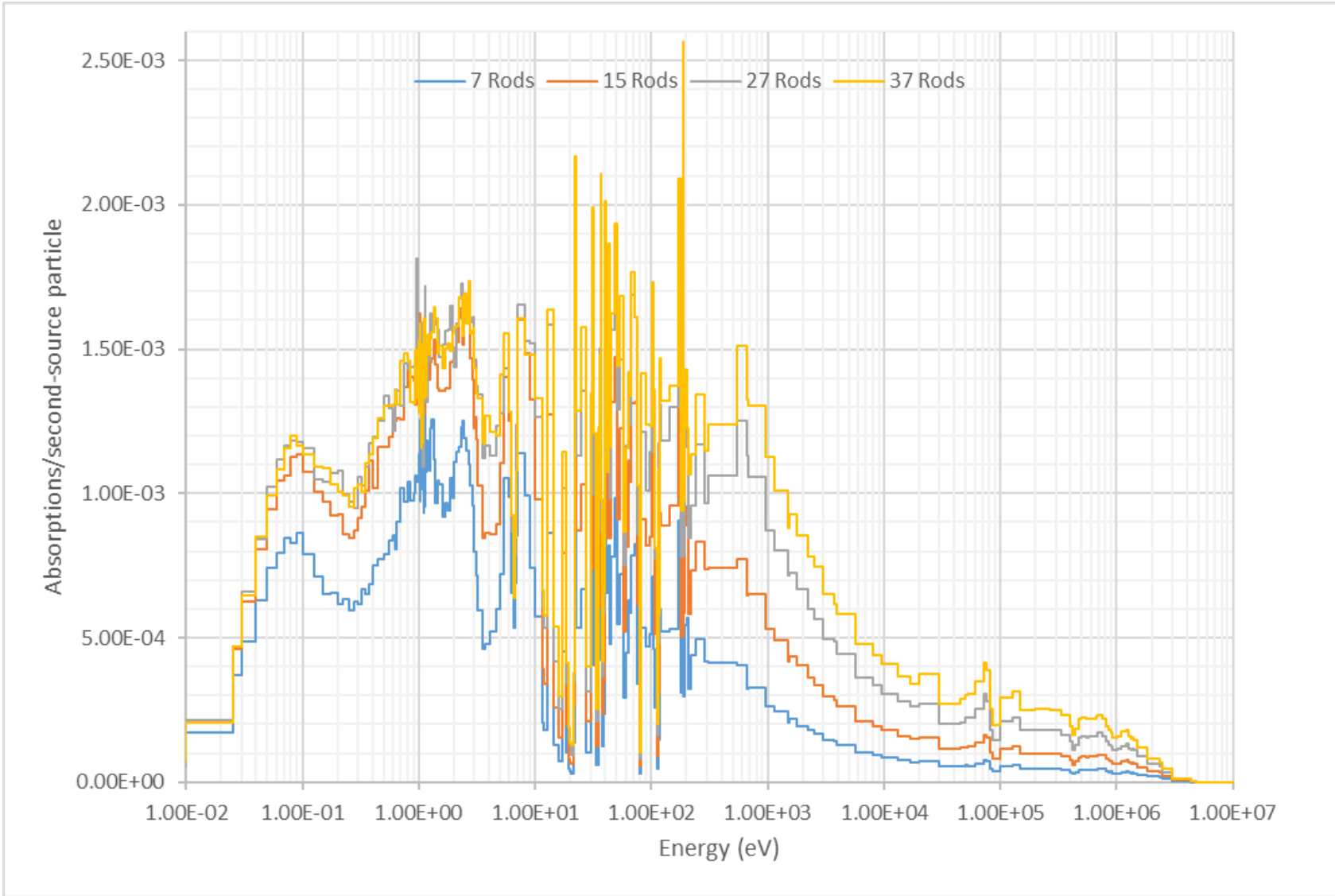


Fig. 8. Energy-dependent reaction rate for a variable number of Hf rods.

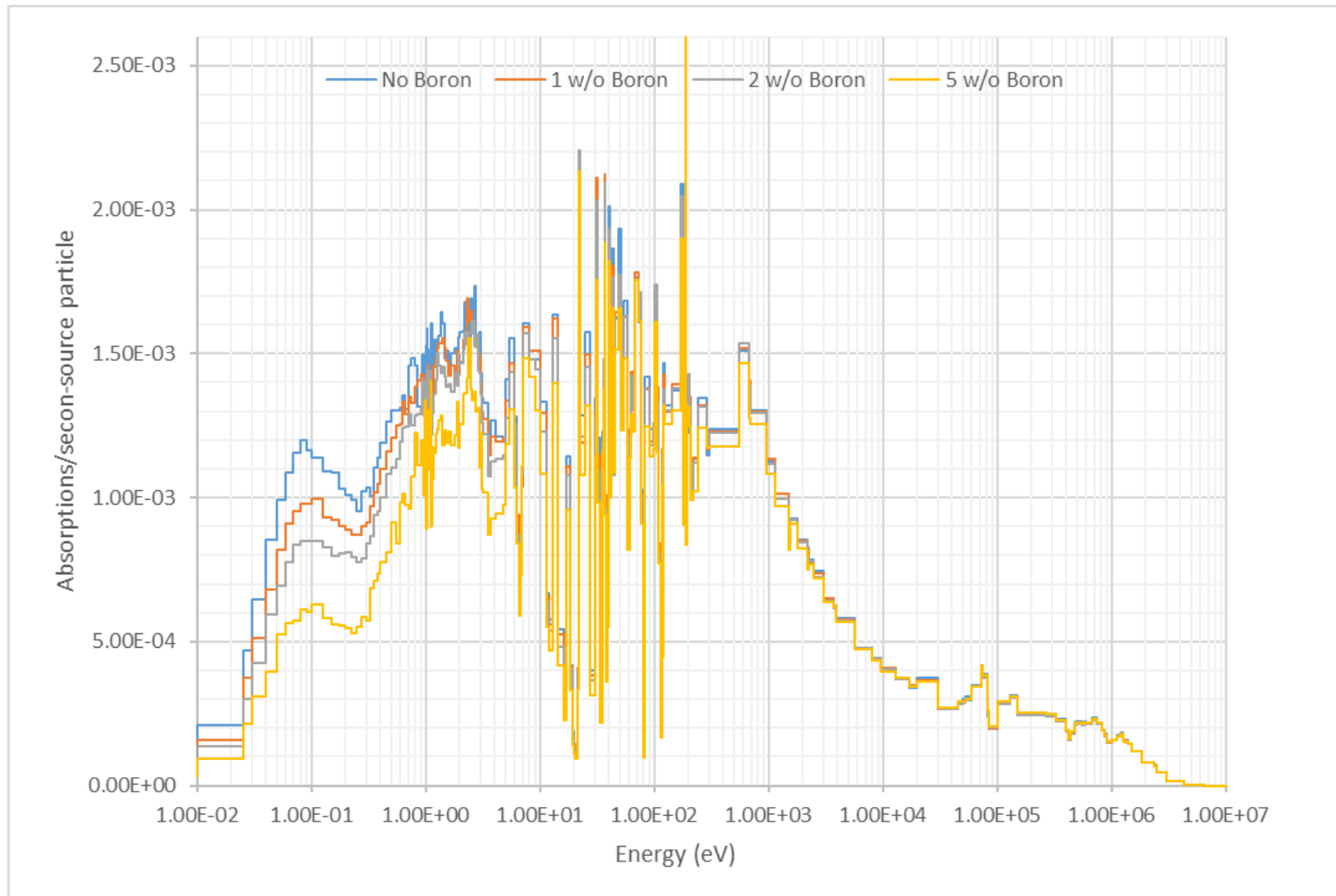


Fig. 9. Energy-dependent reaction rate for 37 Hf rods in a central aluminum block with a variable amount of boron.

3.3 SILVER

Silver is a strong absorber used in nuclear applications as a control material. This isotopic composition of natural silver is 51.4 wt% ^{107}Ag and 48.2 wt% ^{109}Ag . A plot of the absorption cross section for these isotopes is included in Fig. 10. The absorption reaction rate for Ag is plotted as a function of energy in Fig. 11 for an unborated test region including 7, 15, 27, and 37 test samples, and Fig. 12 shows the energy-dependent absorption reaction rate for an aluminum test region with 37 test samples and boron concentrations of 0, 1, 2, and 5 wt%. Table 5 shows the few-group absorption reaction rates as a percentage of the total absorptions for each of the above rod configurations. Fig. 11 shows that there is a tendency for the Ag absorption rate to saturate at thermal energies because the reaction rate increases from 27 to 37 samples, but it does not increase thereafter with additional samples. However, the reaction rate increases with additional samples for energies above 10 eV. Fig. 12 shows that the increase in the boron concentration of the central block leads to a significant reduction in the thermal reaction rate, but the reaction rate above the thermal range remains essentially unchanged. Based on these results, it appears that Ag would be a good test material candidate if data about this material are desired.

Table 5. Few group reaction rates for Ag experimental configurations

Number of rods	Boron loading (wt%)	$E < 1 \text{ eV}$ (%)	$1 \text{ eV} < E < 100 \text{ eV}$ (%)	$100 \text{ eV} < E < 1 \text{ keV}$ (%)	$1 \text{ keV} < E < 1 \text{ MeV}$ (%)	$E > 1 \text{ MeV}$ (%)
7	0	39.80	37.41	7.86	14.25	0.68
15	0	35.56	37.17	8.67	17.75	0.84
27	0	31.00	35.64	9.39	22.86	1.10
37	0	27.97	34.14	9.86	26.75	1.28
37	1	24.81	34.94	10.59	28.31	1.36
37	2	22.49	35.43	11.04	29.61	1.42
37	5	18.27	35.38	11.97	32.80	1.58

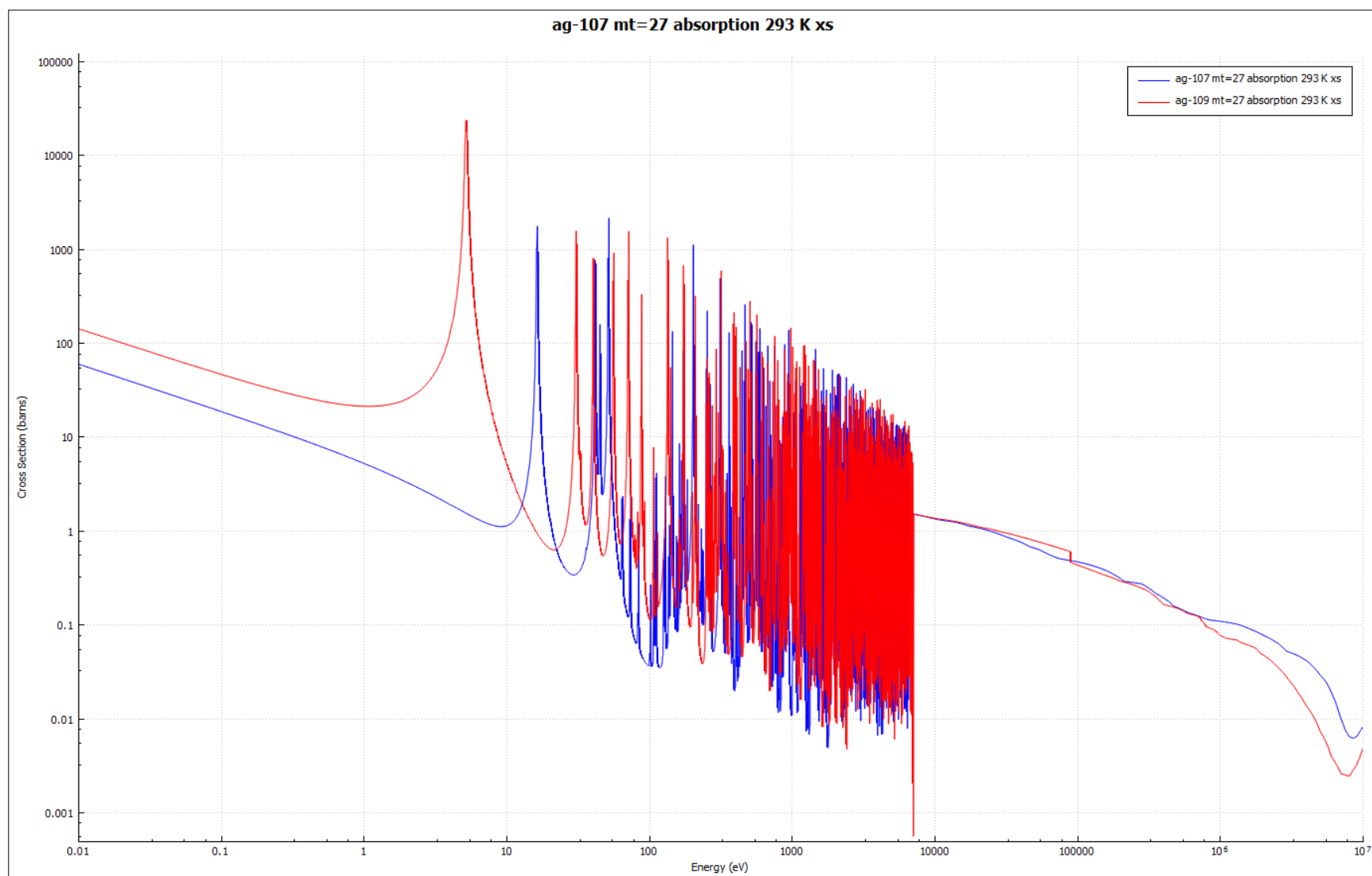


Fig. 10. Energy-dependent absorption cross section for major (>5 wt%) Ag isotopes.

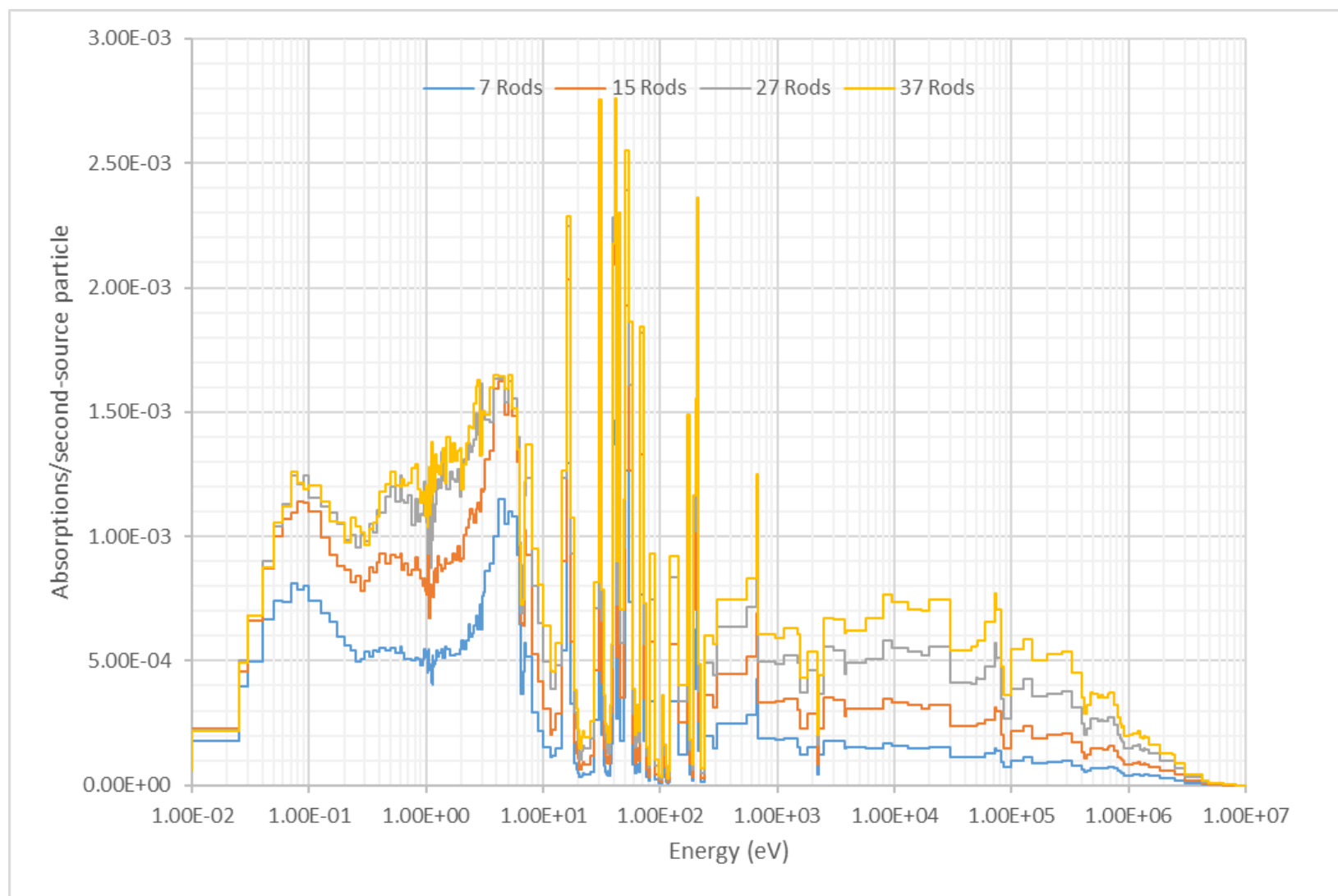


Fig. 11. Energy-dependent reaction rate for a variable number of Ag rods.

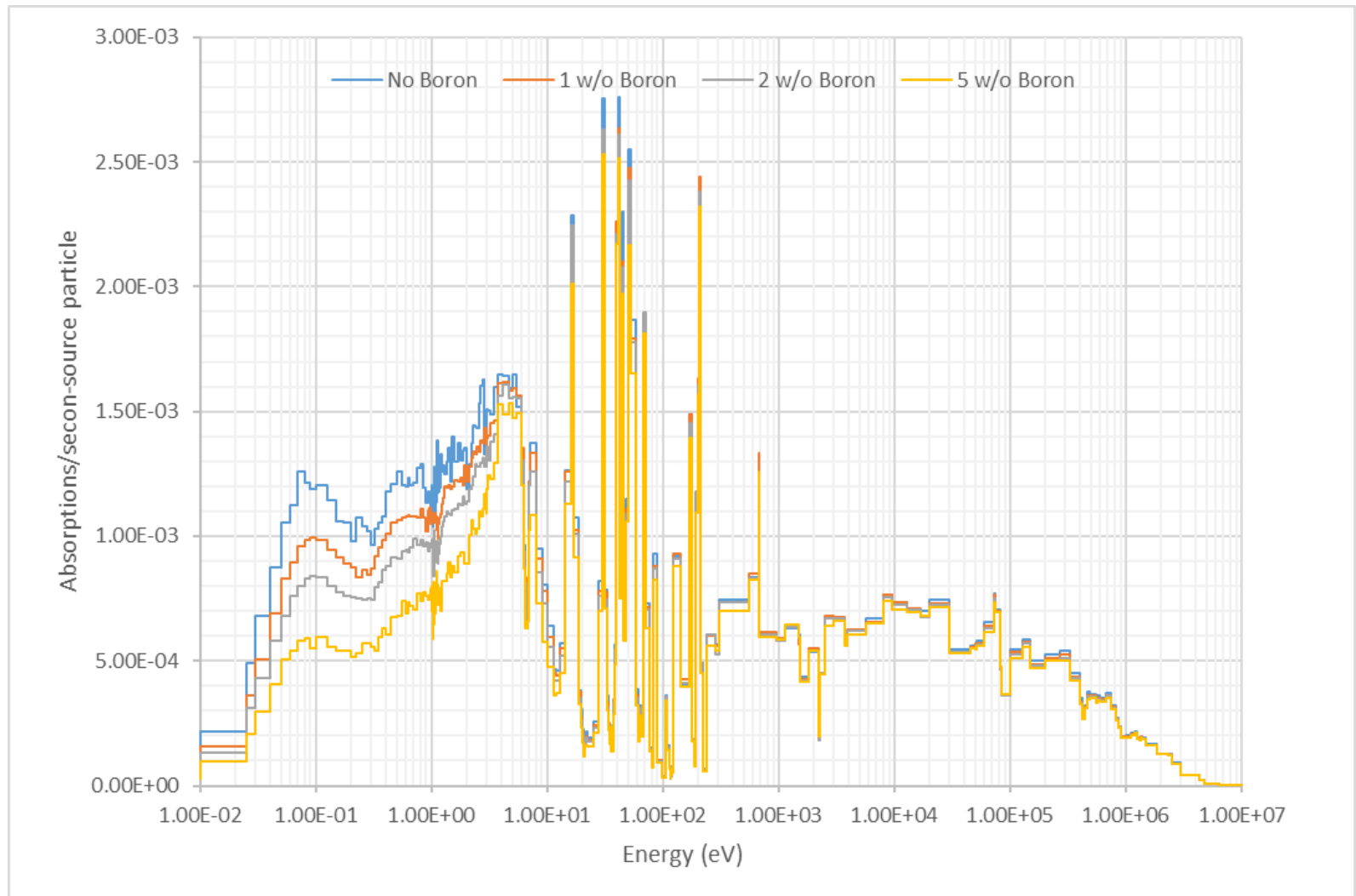


Fig. 12. Energy-dependent reaction rate for ^{37}Ag rods in a central aluminum block with a variable amount of boron.

3.4 TANTALUM

Tantalum (Ta) is a neutron absorber used as a structural material in nuclear applications. Tantalum is nearly isotopically pure, with 99.99 wt% of natural tantalum being composed of ^{181}Ta . The cross section from ^{181}Ta is plotted in Fig. 13. The absorption reaction rate for Ta is plotted as a function of energy in Fig. 14 for an unborated test block including 7, 15, 27, and 37 test samples, and Fig. 15 shows the energy-dependent absorption reaction rate for an aluminum block with 37 test samples and boron concentrations of 0, 1, 2, and 5 wt%. Table 6 presents the few-group absorption reaction rates as a percentage of the total absorptions for each of the rod configurations. Fig. 14 shows a moderate tendency for the Ta absorption rate to saturate at thermal energies because the reaction rate increases from 7 to 27 samples, but it does not increase substantially thereafter with additional samples. However, the reaction rate increases with additional samples for energies above 10 eV. Fig. 15 shows that the increase in the boron concentration of the central block leads to a significant reduction in the thermal reaction rate, but the reaction rate above the thermal range remains essentially unchanged. Based on these results, it appears that Ta would be a good test material candidate if data about this material is desired.

Table 6. Few-group reaction rates for Ta experimental configurations

Number of rods	Boron loading (wt%)	$E < 1 \text{ eV}$ (%)	$1 \text{ eV} < E < 100 \text{ eV}$ (%)	$100 \text{ eV} < E < 1 \text{ keV}$ (%)	$1 \text{ keV} < E < 1 \text{ MeV}$ (%)	$E > 1 \text{ MeV}$ (%)
7	0	21.13	29.77	26.02	22.19	0.89
15	0	19.30	27.42	27.24	25.02	1.01
27	0	17.45	24.13	28.36	28.87	1.19
37	0	16.00	22.38	28.85	31.46	1.31
37	1	11.99	22.84	30.68	33.12	1.38
37	2	9.88	22.82	31.75	34.13	1.42
37	5	6.72	21.94	33.37	36.45	1.51

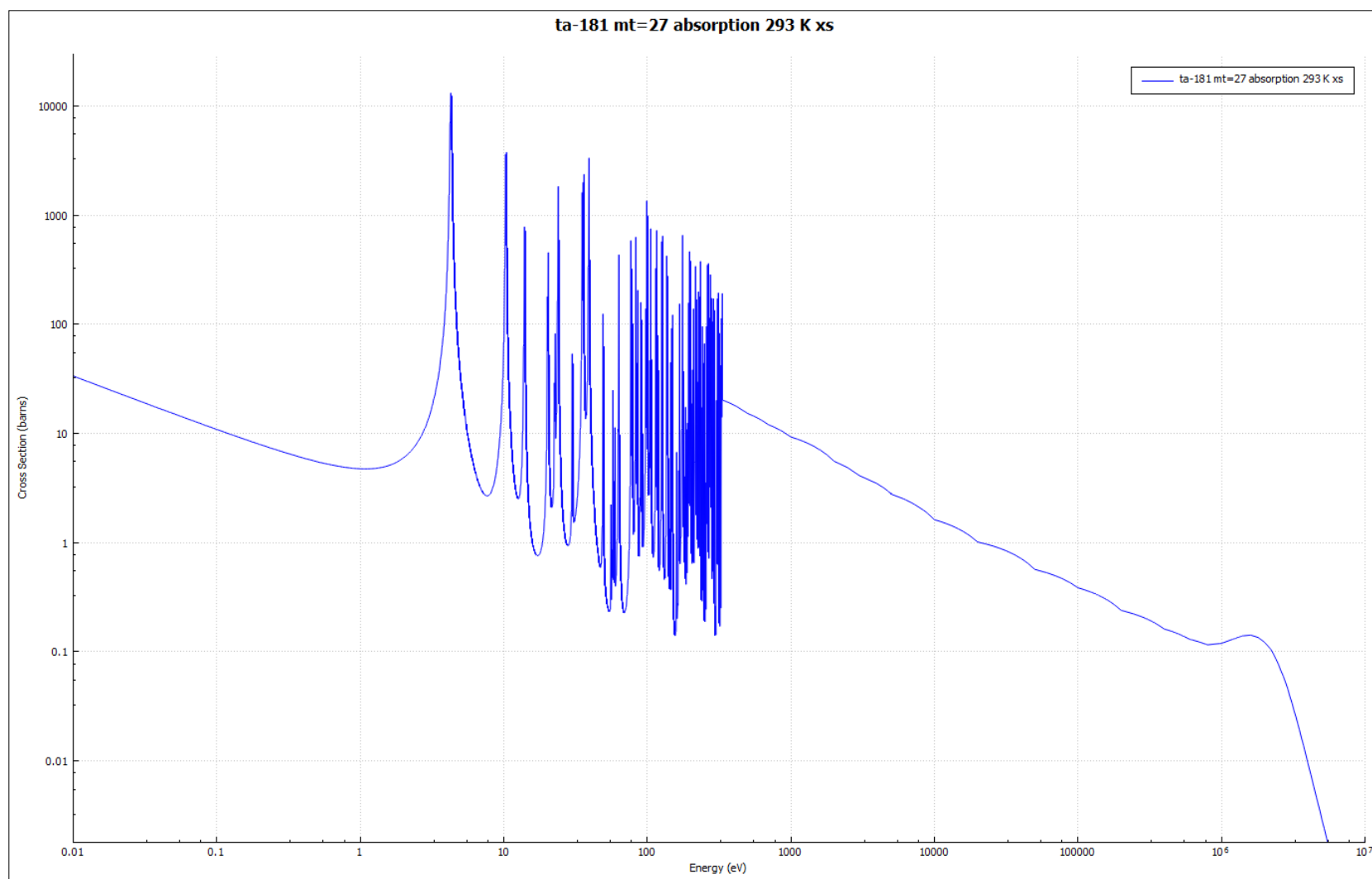


Fig. 13. Energy-dependent absorption cross section for ^{181}Ta .

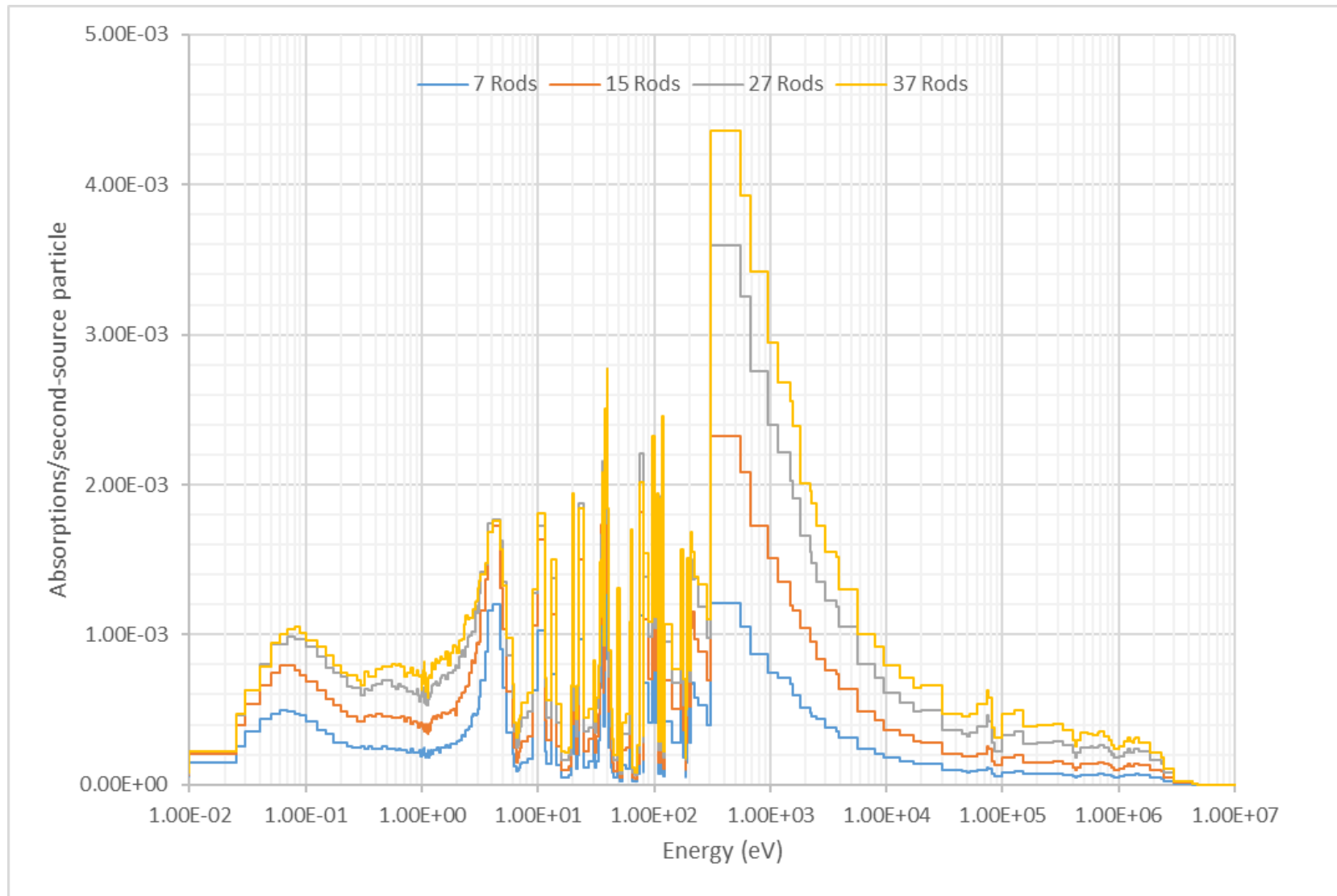


Fig. 14. Energy-dependent reaction rate for a variable number of Ta rods.

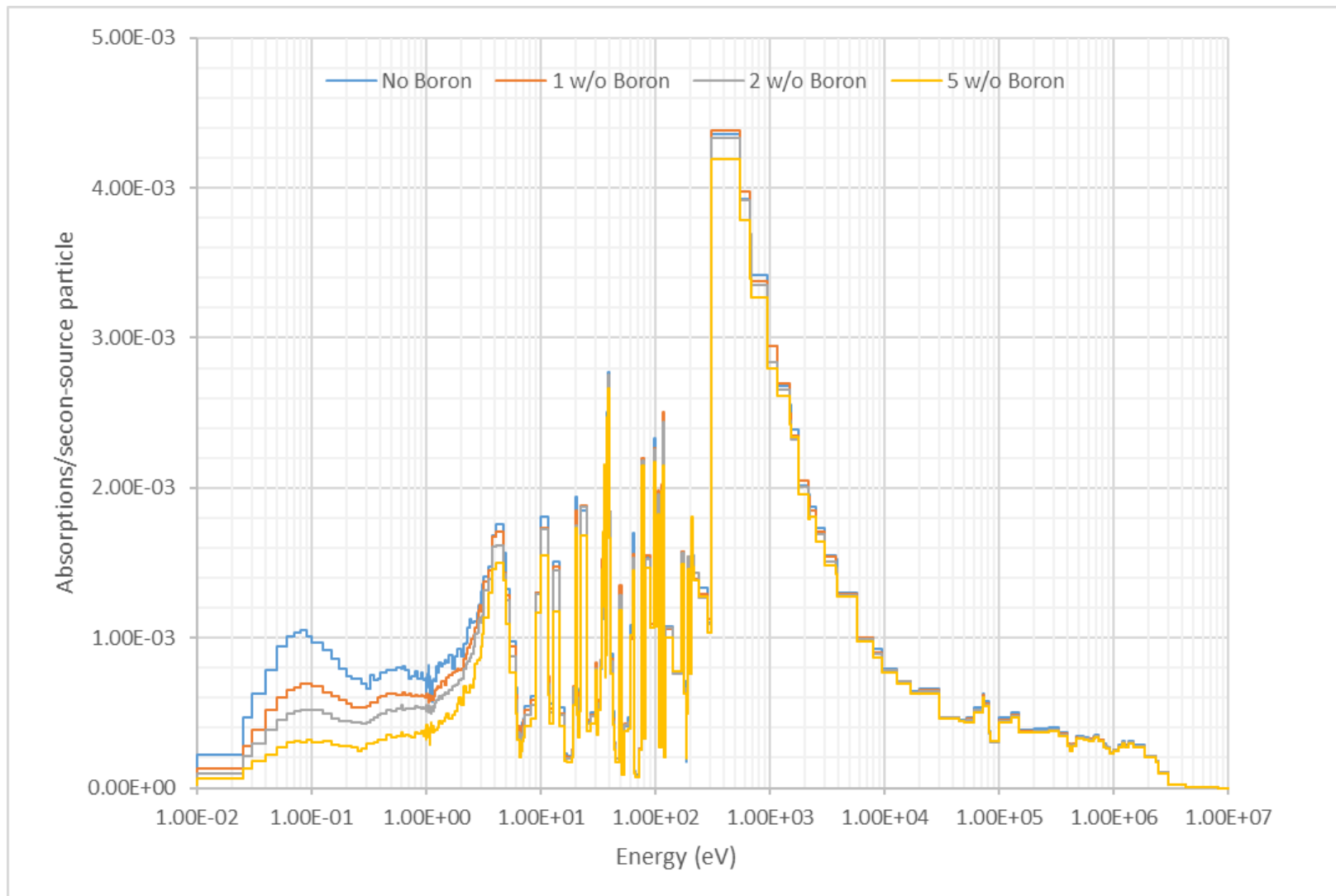


Fig. 15. Energy-dependent reaction rate for 37 Ta rods in a central aluminum block with a variable amount of boron.

3.5 INDIUM

Indium is a neutron-absorbing material typically used as a control material. The isotopic composition of natural indium is 4.3 wt% ^{113}In and 95.7 wt% ^{115}In . In Fig. 17, the absorption reaction rate for In is plotted as a function of energy for an unborated test block including 7, 15, 27, and 37 test samples, and Fig. 18 shows the energy-dependent absorption reaction rate for an aluminum block with 37 test samples and boron concentrations of 0, 1, 2, and 5 wt%. Table 7 shows the few-group absorption reaction rates as a percentage of the total absorptions for each of the rod configurations specified. Fig. 17 shows a strong tendency for the In absorption rate to saturate at thermal energies because the reaction rate increases from 7 to 15 samples, but with additional samples, it does not increase substantially thereafter. However, there is an increase in the reaction rate with additional samples for energies above 10 eV. Fig. 18 shows that the increase in the boron concentration of the central block leads to a significant reduction in the thermal reaction rate, but the reaction rate above the thermal range remains essentially unchanged. Based on these results, it appears that In would be a good test material candidate if data about this material are desired.

Table 7. Few group reaction rates for In experimental configurations

Number of rods	Boron loading (wt%)	$E < 1 \text{ eV}$ (%)	$1 \text{ eV} < E < 100 \text{ eV}$ (%)	$100 \text{ eV} < E < 1 \text{ keV}$ (%)	$1 \text{ keV} < E < 1 \text{ MeV}$ (%)	$E > 1 \text{ MeV}$ (%)
7	0	50.61	32.33	5.90	10.24	0.91
15	0	44.75	32.95	7.05	14.01	1.24
27	0	37.95	32.51	8.32	19.46	1.74
37	0	34.20	31.05	9.13	23.49	2.13
37	1	32.00	31.62	9.55	24.58	2.25
37	2	30.50	31.79	9.84	25.53	2.34
37	5	27.18	31.48	10.75	28.01	2.57

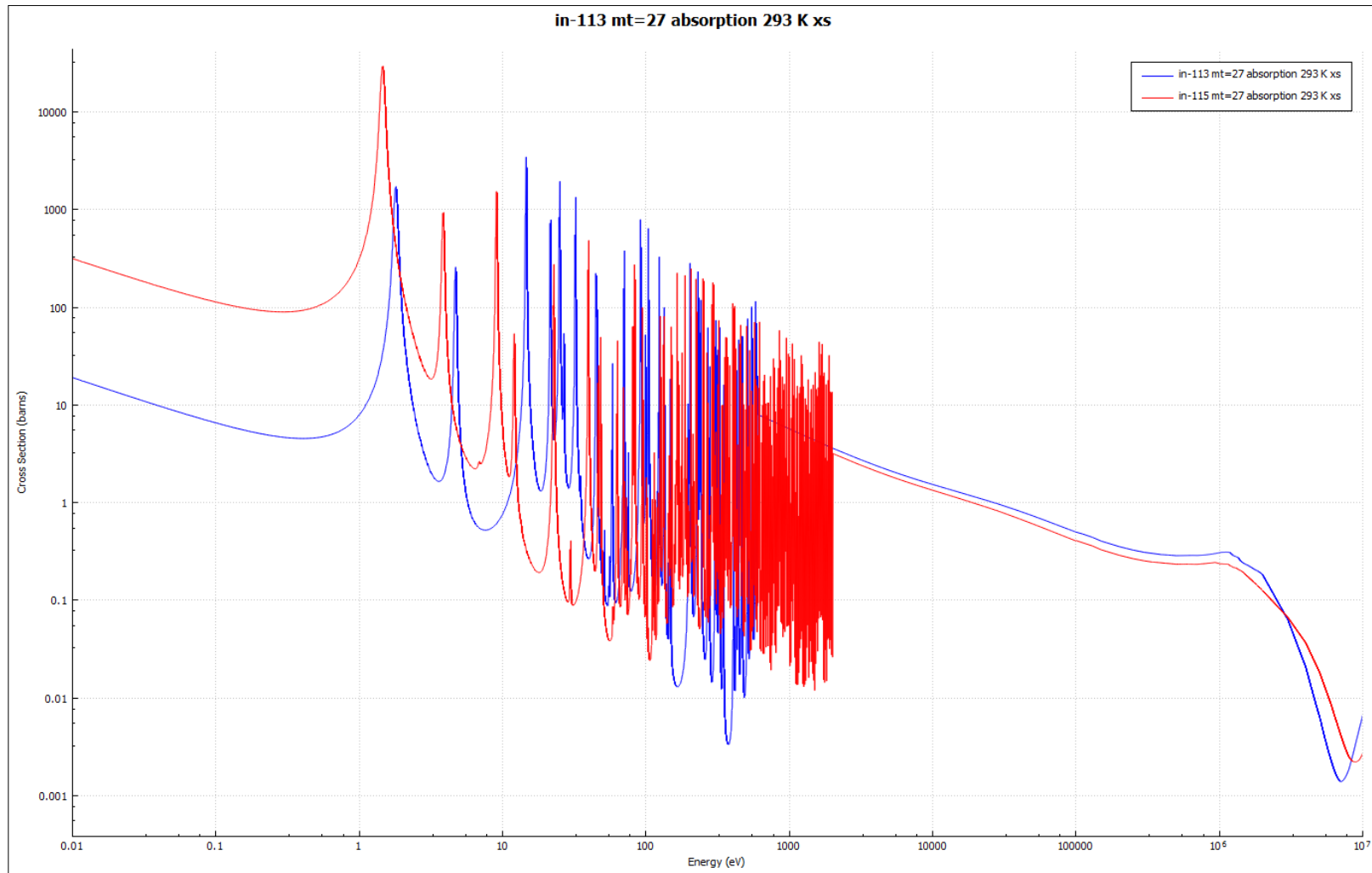


Fig. 16. Energy-dependent absorption cross section for major (>5 wt%) In isotopes.

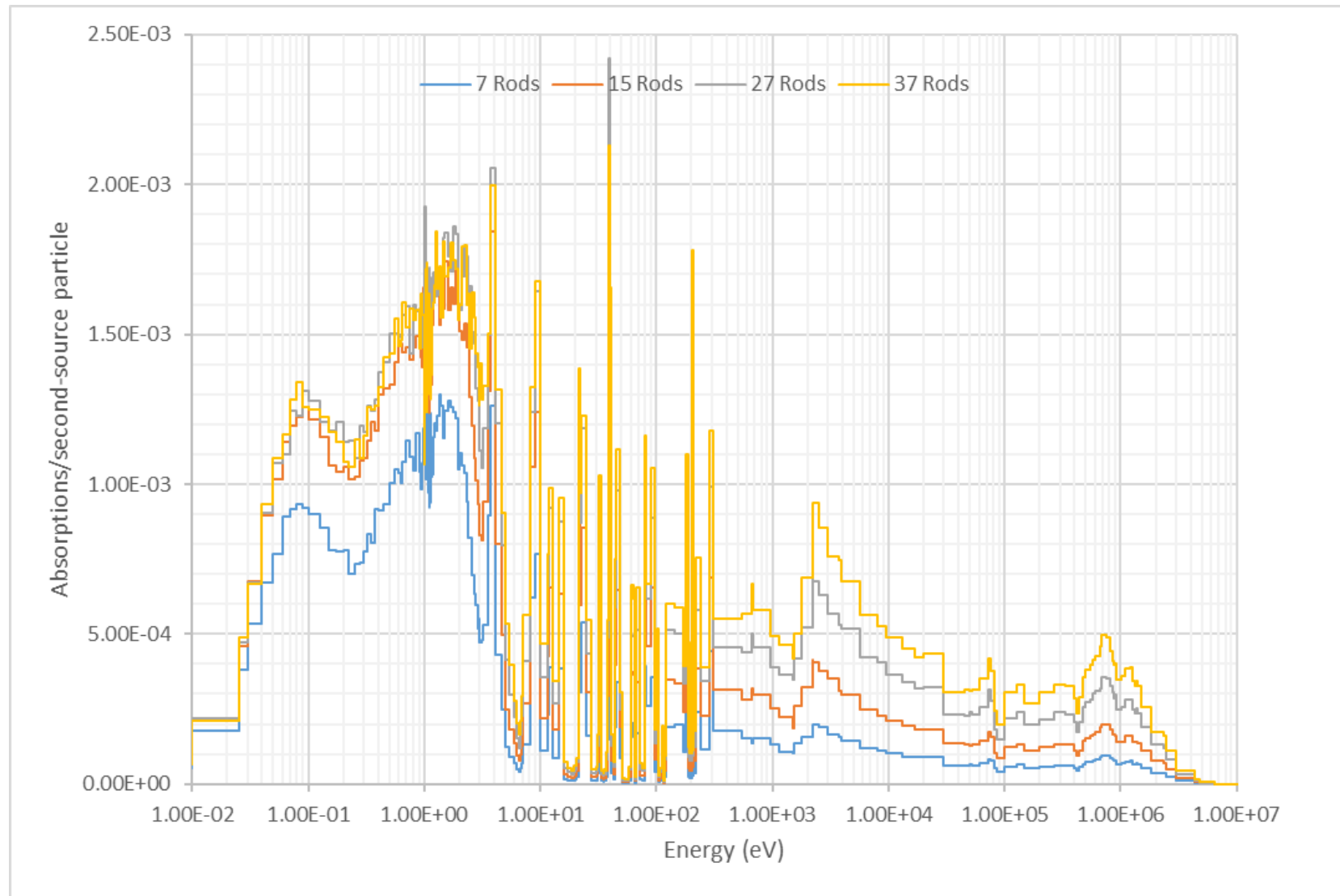


Fig. 17. Energy-dependent reaction rate for a variable number of In rods.

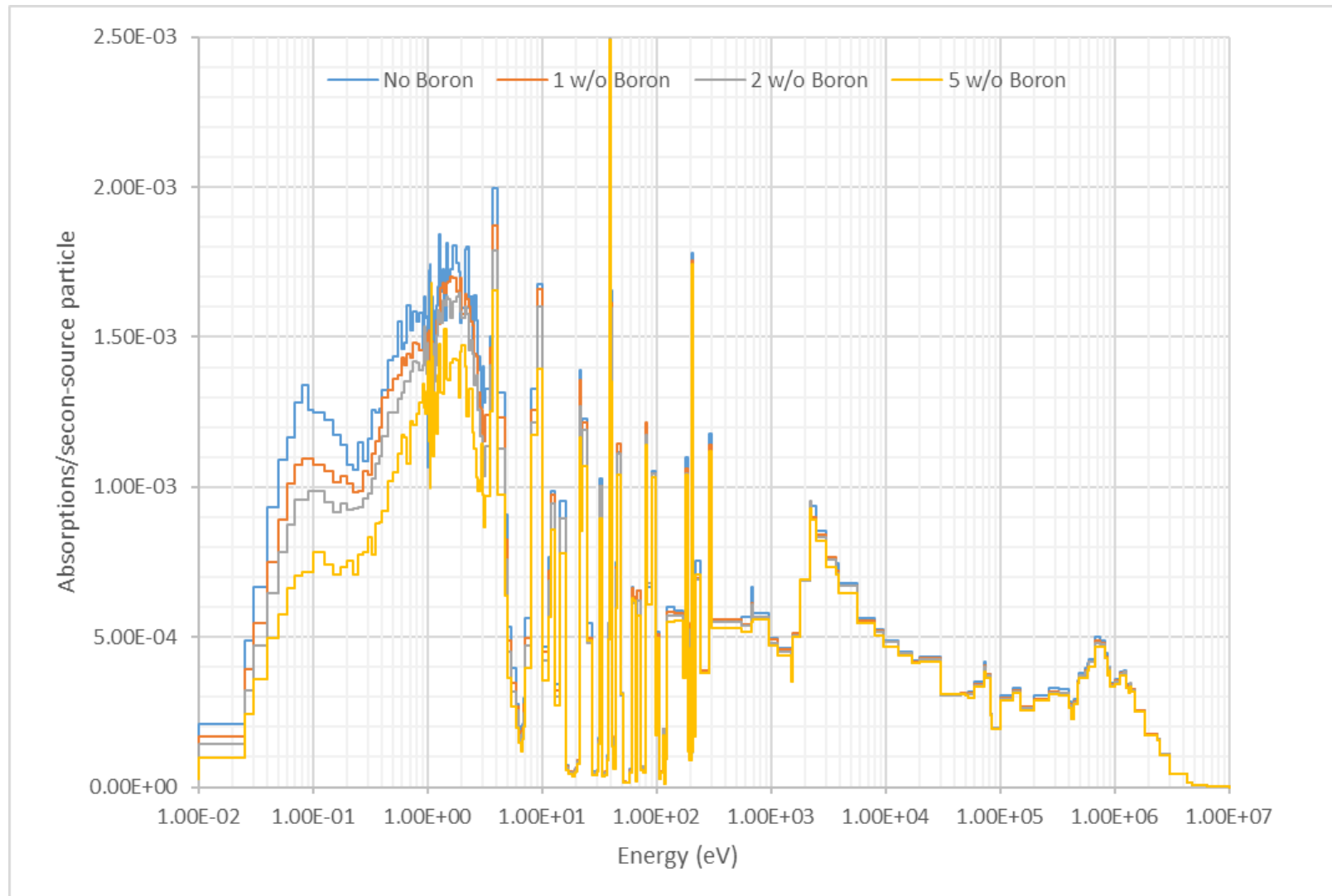


Fig. 18. Energy-dependent reaction rate for ^{37}In rods in a central aluminum block with a variable amount of boron.

3.6 COBALT

Cobalt is a structural material commonly used in nuclear applications. Cobalt is isotopically pure, with 100 wt% of natural cobalt being ^{59}Co . The absorption cross section for the ^{59}Co is plotted in Fig. 19. In Fig. 20, the absorption reaction rate for Co is plotted as a function of energy for an unborated test block including 7, 15, 27, and 37 test samples, and Fig. 21 shows the energy-dependent absorption reaction rate for an aluminum block, with 37 test samples and boron concentrations of 0, 1, 2, and 5 wt%. Table 8 shows the few-group absorption reaction rates a percentage of the total absorptions for each of the rod configurations. Fig. 20 shows a mild tendency for the Co absorption rate to saturate at thermal energies because the reaction rate increases from 7 to 27 samples, but with additional samples it does increase moderately thereafter. Unlike the previous elements studied, the saturation effect is evident across the energy spectrum. Fig. 21 shows that the increase in the boron concentration of the central block does lead to a significant reduction in the thermal reaction rate, however, the reaction rate above the thermal range remains essentially unchanged. Based on these results, it appears that Co would be a moderately good test material candidate if data about this material are desired. It is noted that the worth of the 37 sample Co loading for the 5 wt% borated aluminum block drops to $0.00343 \Delta k_{\text{eff}}$, which means that information could be derived from this central block because it would not likely be possible to load it with a significantly smaller sample. It may be desirable to decrease the largest boron concentration in the test region for this material if it is needed.

Table 8. Few-group reaction rates for Co experimental configurations

Number of rods	Boron loading (wt%)	$E < 1 \text{ eV}$ (%)	$1 \text{ eV} < E < 100 \text{ eV}$ (%)	$100 \text{ eV} < E < 1 \text{ keV}$ (%)	$1 \text{ keV} < E < 1 \text{ MeV}$ (%)	$E > 1 \text{ MeV}$ (%)
7	0	56.88	29.22	12.27	1.48	0.14
15	0	51.82	33.81	12.42	1.77	0.18
27	0	46.21	39.07	12.26	2.23	0.23
37	0	42.97	41.95	12.15	2.64	0.27
37	1	39.07	44.09	13.60	2.94	0.30
37	2	36.32	45.43	14.75	3.17	0.33
37	5	31.43	47.08	17.30	3.79	0.40

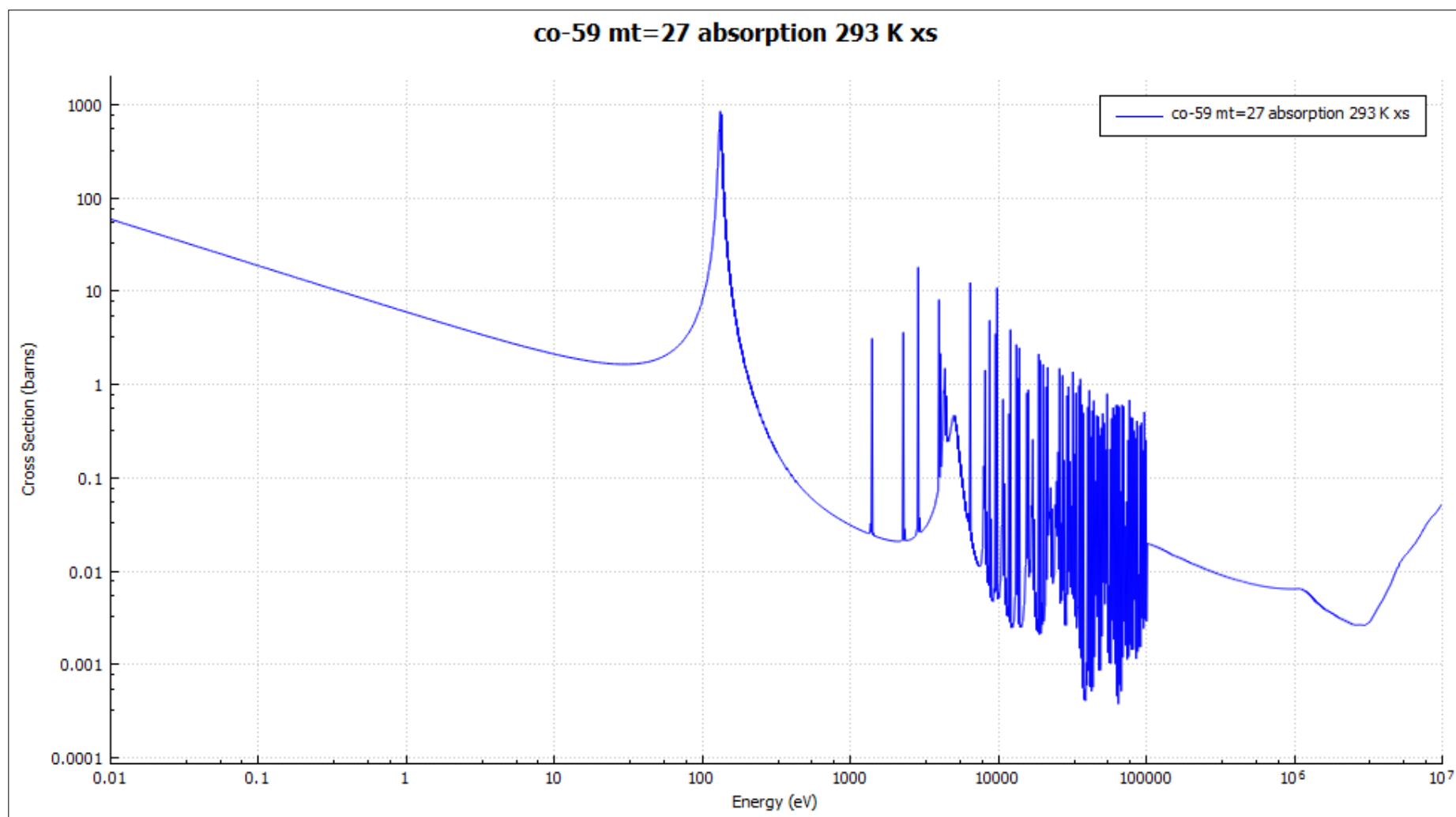


Fig. 19. Energy-dependent absorption cross section for ^{60}Co .

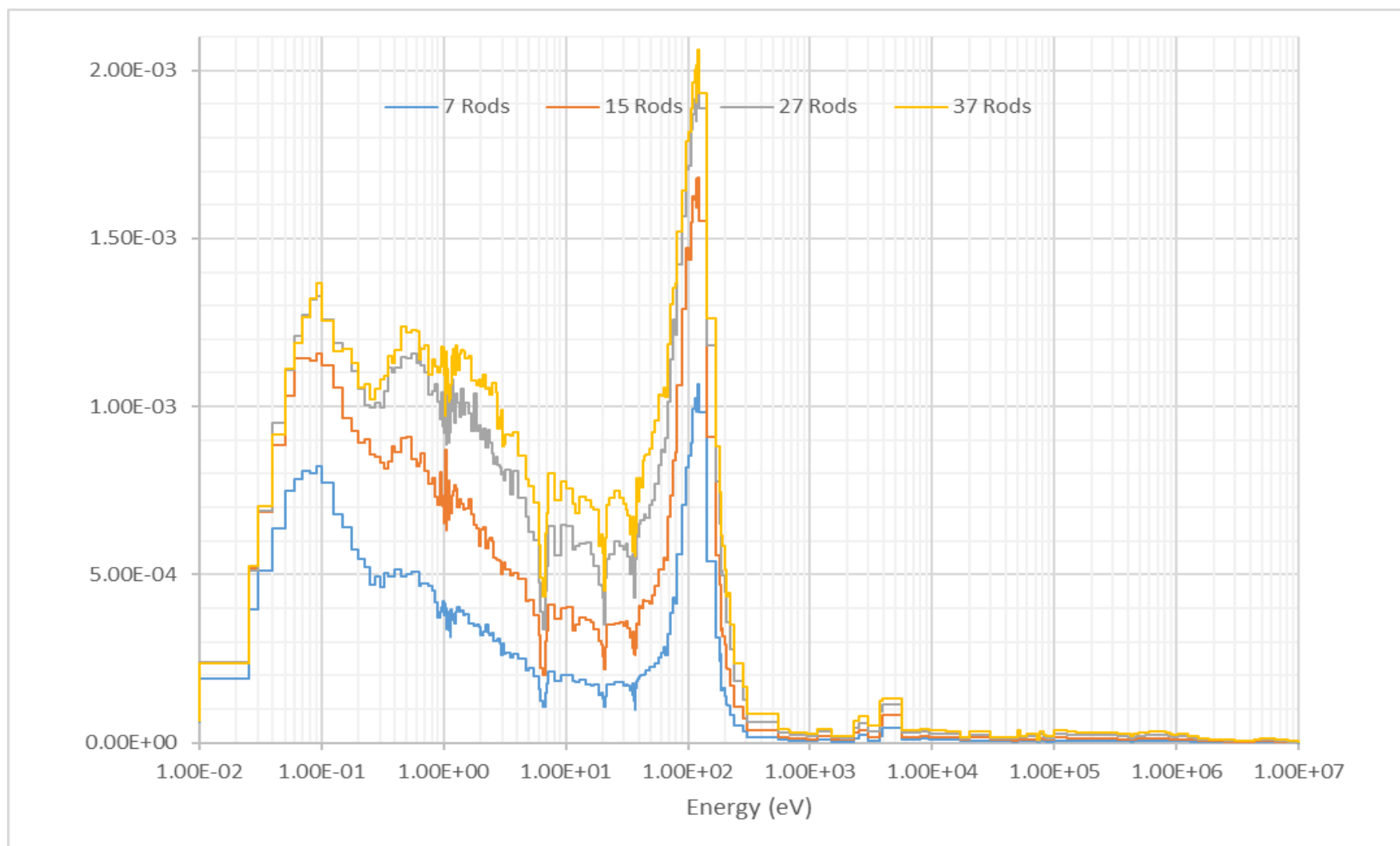


Fig. 20. Energy-dependent reaction rate for a variable number of Co rods.

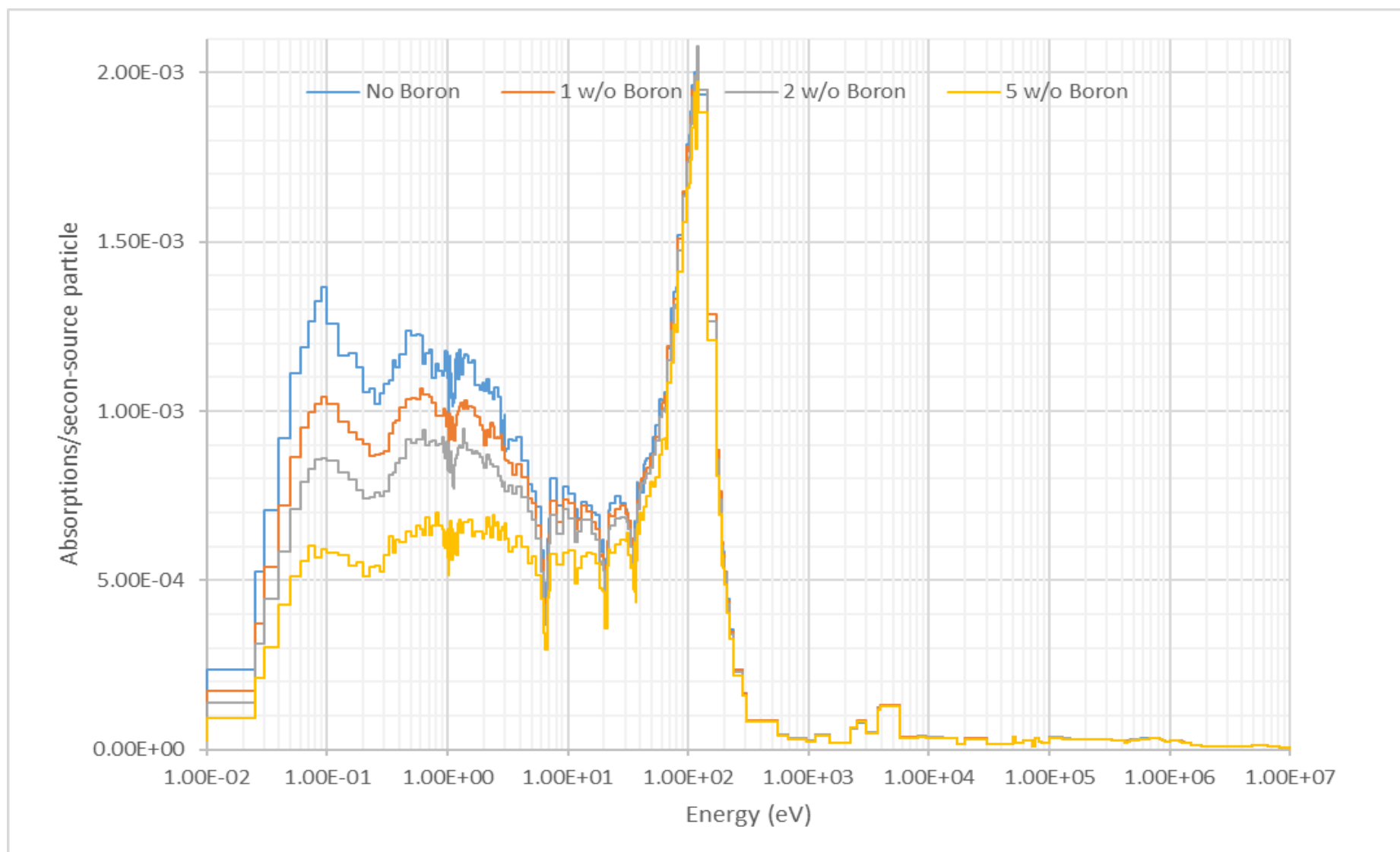


Fig. 21. Energy-dependent reaction rate for ^{37}Co rods in a central aluminum block with a variable amount of boron.

3.7 TUNGSTEN

Tungsten (W) is a structural material commonly used in nuclear applications. This isotopic composition of natural W is 26.5 wt% ^{182}W , 14.3 wt% ^{183}W , 30.64 wt% ^{184}W , and 28.4 wt% ^{186}W . A plot of the absorption cross section for these isotopes is included in Fig. 22. The absorption reaction rate for W is plotted as a function of energy in Fig. 23 for an unborated test block including 7, 15, 27, and 37 test samples, and the energy-dependent absorption reaction rate is shown in Fig. 24 for an aluminum block with 37 test samples and boron concentrations of 0, 1, 2, and 5 wt%. Table 9 shows the few-group absorption reaction rates as a percentage of the total absorptions for each of the rod configurations. Fig. 23 shows a mild tendency for the W absorption rate to saturate at thermal energies because the reaction rate increases from 7–27 samples, but it only moderately increases thereafter with additional samples. Fig. 24 shows that the increase in the boron concentration of the central block leads to a substantial reduction in the thermal reaction rate, but the reaction rate above the thermal range remains essentially unchanged. Based on these results, it appears that W would be a moderately good test material candidate if data about this material are desired.

Table 9. Few-group reaction rates for W experimental configurations

Number of rods	Boron loading (wt%)	$E < 1 \text{ eV}$ (%)	$1 \text{ eV} < E < 100 \text{ eV}$ (%)	$100 \text{ eV} < E < 1 \text{ keV}$ (%)	$1 \text{ keV} < E < 1 \text{ MeV}$ (%)	$E > 1 \text{ MeV}$ (%)
7	0	34.79	40.84	12.74	10.74	0.89
15	0	33.48	39.61	13.33	12.53	1.04
27	0	32.02	37.46	13.91	15.36	1.25
37	0	30.31	36.33	14.11	17.85	1.41
37	1	23.84	38.88	15.89	19.83	1.56
37	2	20.10	39.97	17.01	21.24	1.68
37	5	14.24	39.79	19.09	24.90	1.98

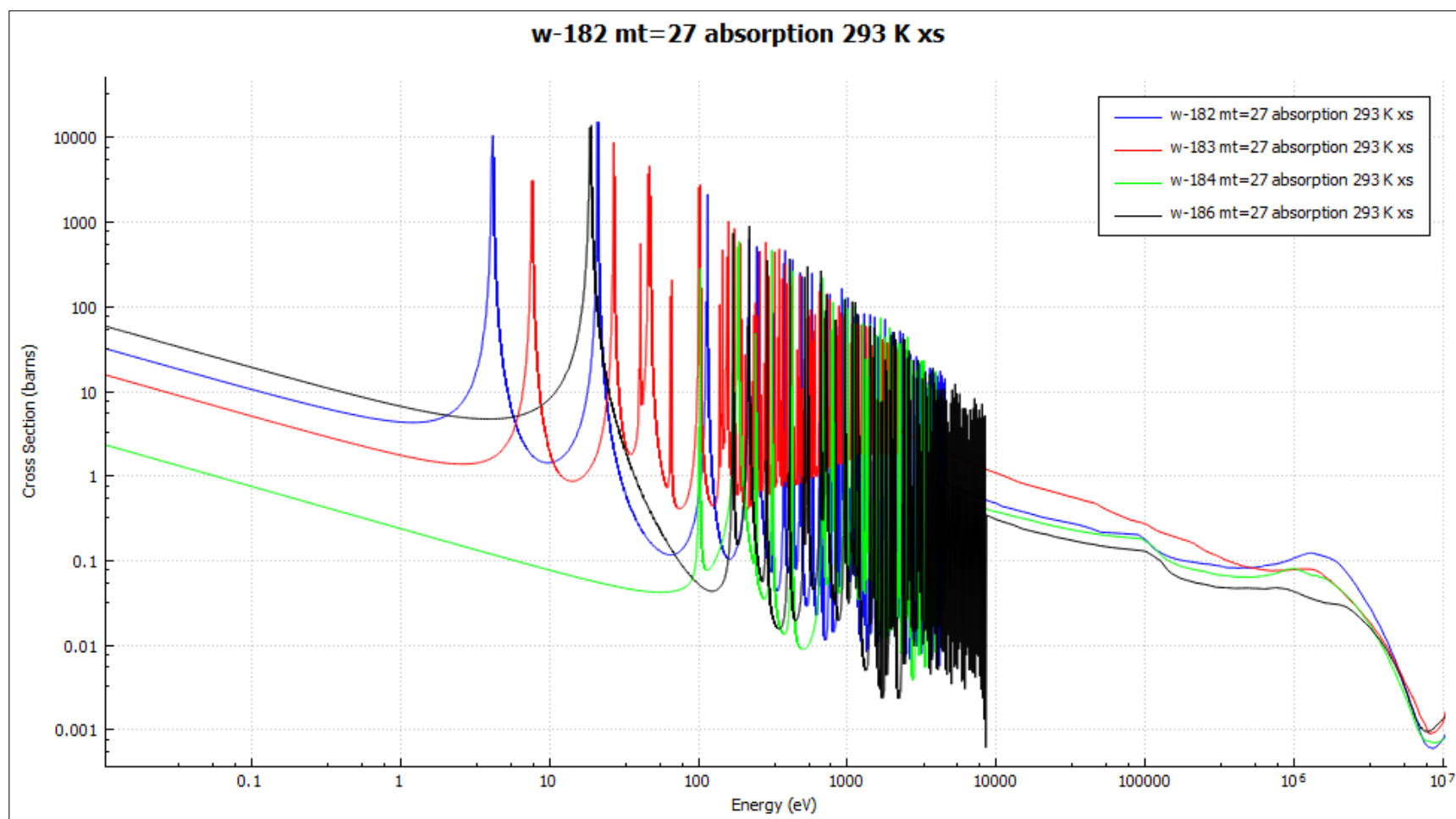


Fig. 22. Energy-dependent absorption cross section for major (>5 wt%) W isotopes.

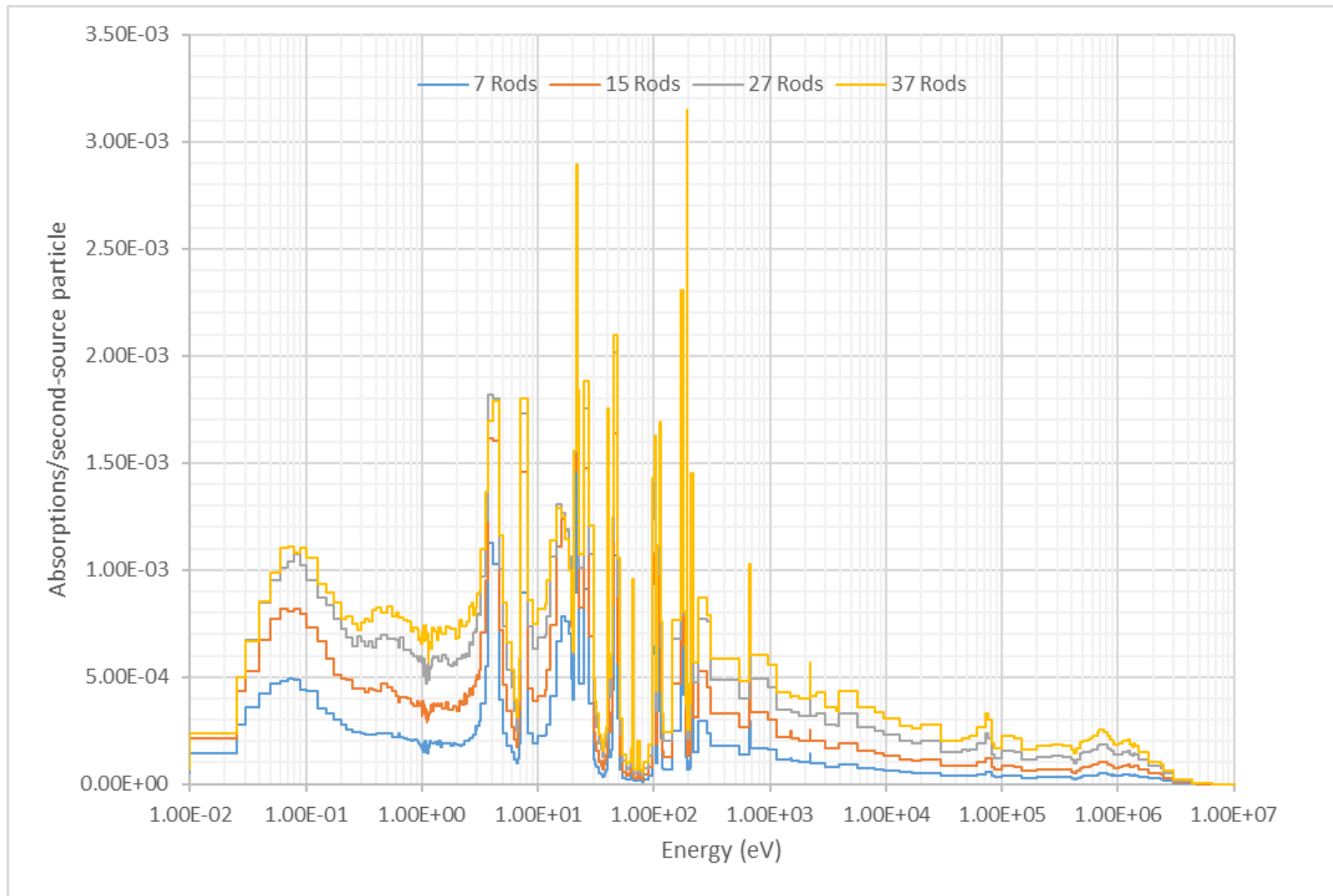


Fig. 23. Energy-dependent reaction rate for a variable number of W rods.

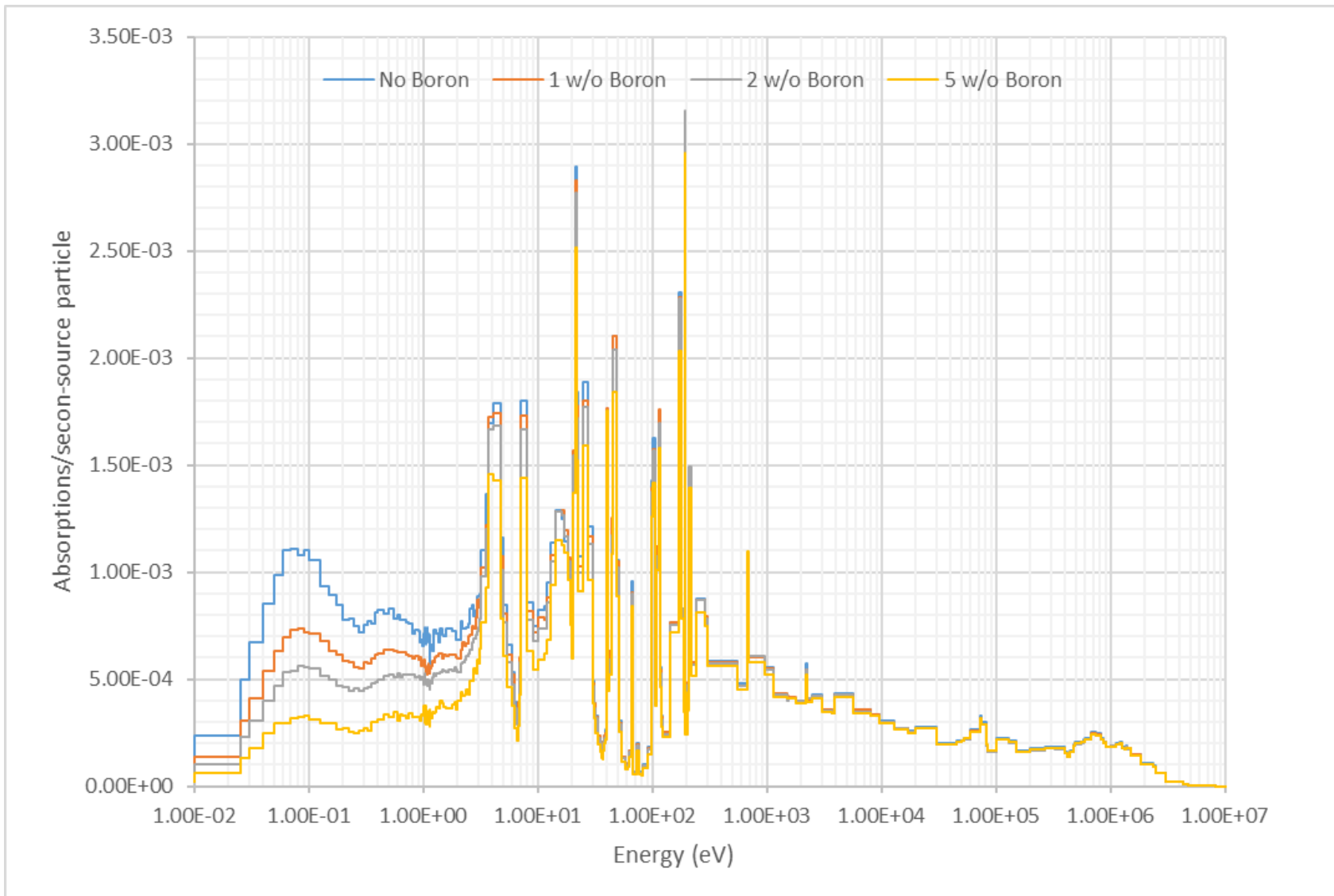


Fig. 24. Energy-dependent reaction rate for 37 W rods in a central aluminum block with a variable amount of boron.

3.8 MANGANESE

Manganese (Mn) is a structural material that is commonly used in nuclear applications. Manganese is isotopically pure with 100 wt% of natural Mn being ^{55}Mn . The absorption cross section for ^{55}Mn is plotted in Fig. 25. The absorption reaction rate for ^{55}Mn is plotted as a function of energy in Fig. 26 for an unborated test block including 7, 15, 27, and 37 test samples, and the energy-dependent absorption reaction rate is shown in Fig. 27 for an aluminum block with 37 test samples and boron concentrations of 0, 1, 2, and 5 wt%. Table 10 shows the few-group absorption reaction rates as a percentage of the total absorptions the rod configurations. Fig. 26 shows that there is almost no tendency for the Mn absorption rate to saturate at thermal energies because the reaction rate increases markedly as the number of samples increases to the maximum of 37. Fig. 27 shows that the increase in the boron concentration of the central block leads to a dramatic reduction in the thermal reaction rate. The worth of the 37 Mn samples loaded in the central block with is only $0.00254 \Delta k_{\text{eff}}$ with a 2 wt% boron concentration in the central region. Based on these results, it appears that Mn would not be a fair test material candidate.

Table 10. Few-group reaction rates for Mn experimental configurations

Number of rods	Boron loading (wt%)	$E < 1 \text{ eV}$ (%)	$1 \text{ eV} < E < 100 \text{ eV}$ (%)	$100 \text{ eV} < E < 1 \text{ keV}$ (%)	$1 \text{ keV} < E < 1 \text{ MeV}$ (%)	$E > 1 \text{ MeV}$ (%)
7	0	50.61	32.33	5.90	10.24	0.91
15	0	44.75	32.95	7.05	14.01	1.24
27	0	37.95	32.51	8.32	19.46	1.74
37	0	34.20	31.05	9.13	23.49	2.13
37	1	32.00	31.62	9.55	24.58	2.25
37	2	30.50	31.79	9.84	25.53	2.34
37	5	27.18	31.48	10.75	28.01	2.57

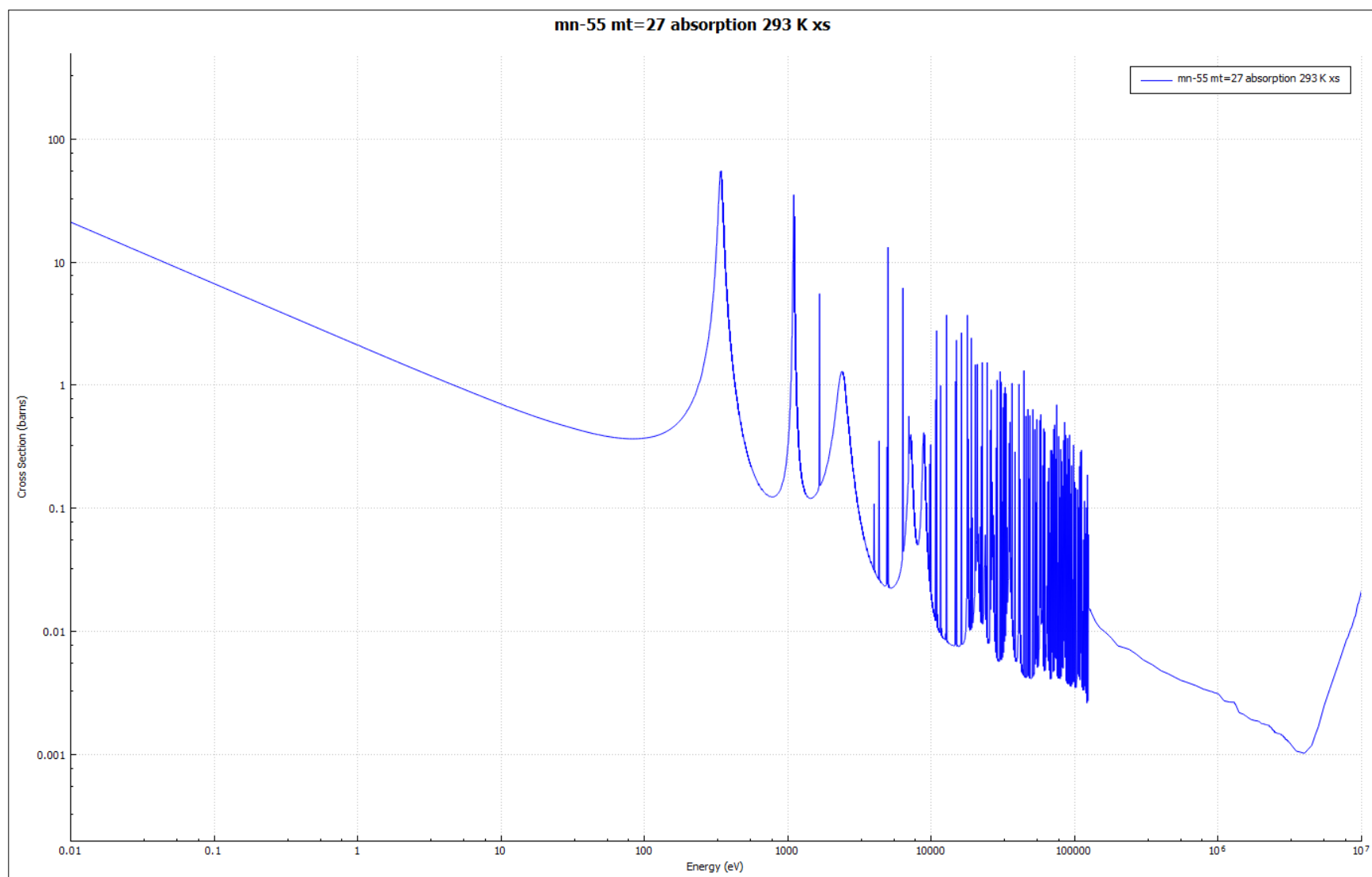


Fig. 25. Energy-dependent absorption cross section for ^{55}Mn .

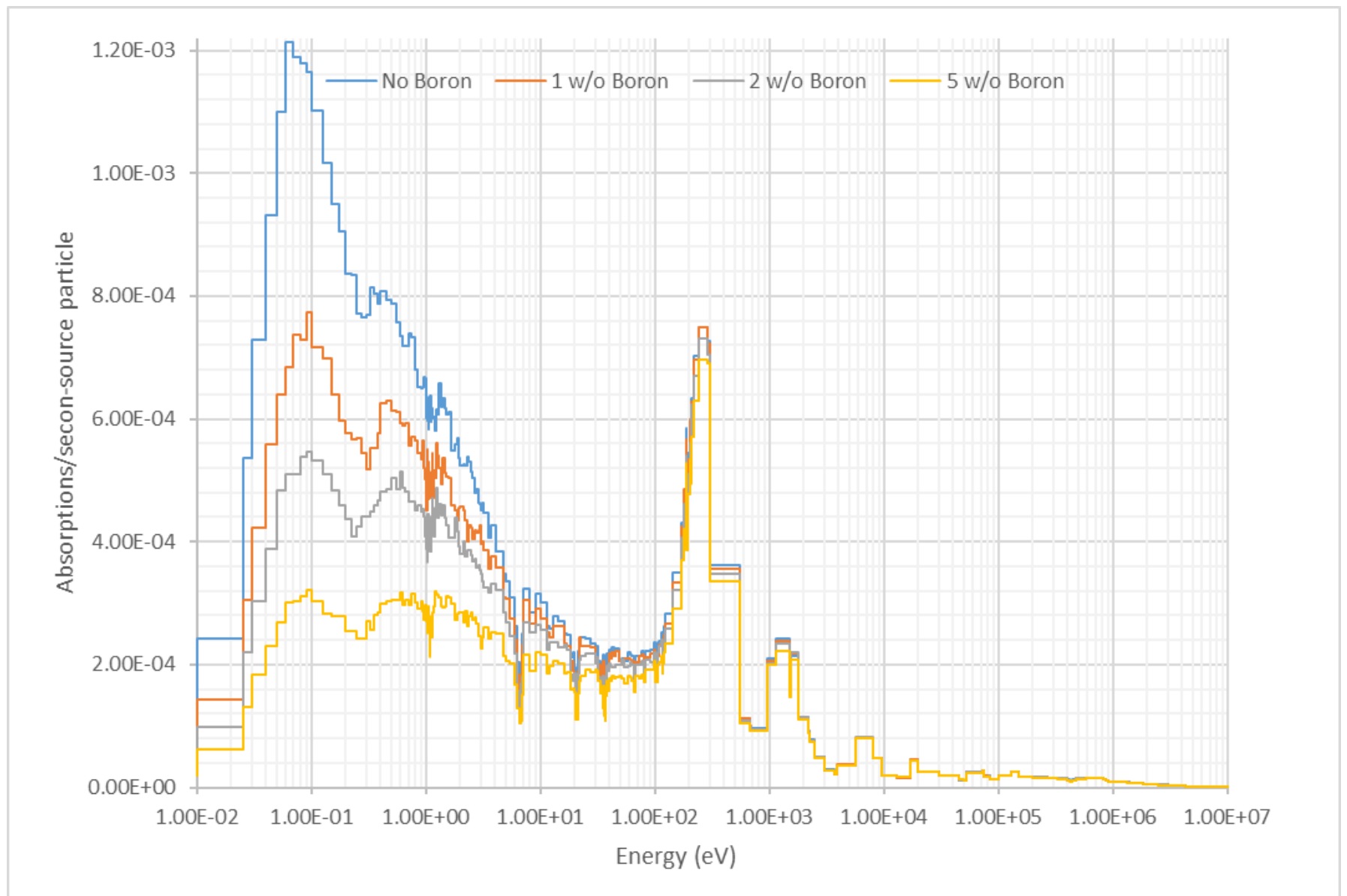


Fig. 26. Energy-dependent reaction rate for a variable number of Mn rods.

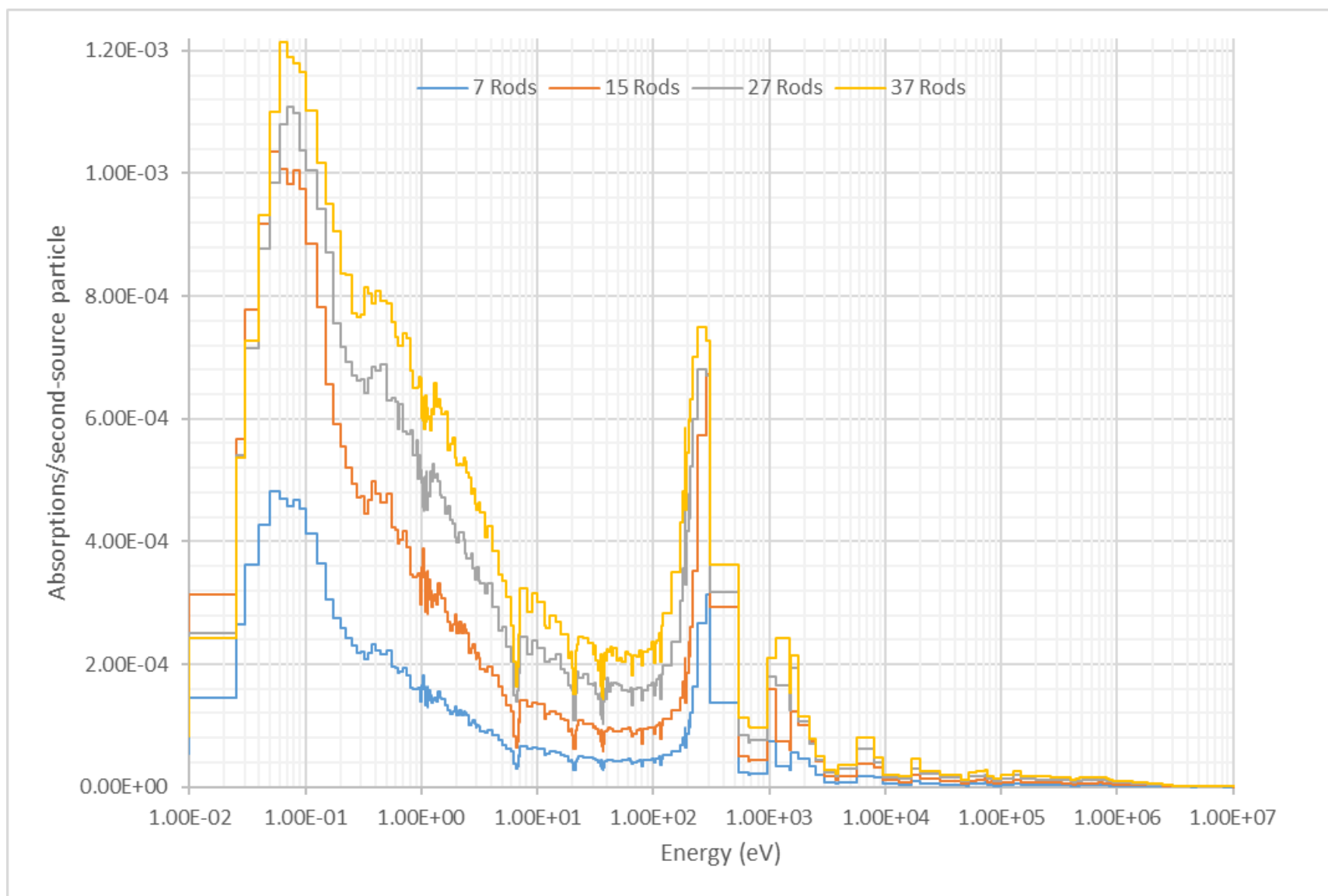


Fig. 27. Energy-dependent reaction rate for ^{37}Mn rods in a central aluminum block with a variable amount of boron.

3.9 ANTIMONY

This isotopic composition of natural antimony (Sb) is 57.2 wt% ^{121}Sb and 42.8 wt% ^{123}Sb . A plot of the absorption cross section for these isotopes is included in Fig. 28. The absorption reaction rate for Sb is plotted as a function of energy in Fig. 29 for an unborated test block that includes 7, 15, 27, and 37 test samples, and the energy-dependent absorption reaction rate is shown in Fig. 30 for an aluminum block with 37 test samples and boron concentrations of 0, 1, 2, and 5 wt%. Table 11 shows the few-group absorption reaction rates as a percentage of the total absorptions for the rod configurations. Fig. 29 shows that there is almost no tendency for the Sb absorption rate to saturate at thermal energies because the reaction rate increases markedly with an increasing number of samples up to the maximum of 37. Fig. 30 shows that the increase in the boron concentration of the central block leads to a significant reduction in the thermal reaction rate, but the reaction rate above the thermal range remains essentially unchanged. Based on these results, it appears that Sb would be a moderately good test material candidate.

Table 11. Few-group reaction rates for Sb experimental configurations

Number of rods	Boron loading (wt%)	$E < 1 \text{ eV}$ (%)	$1 \text{ eV} < E < 100 \text{ eV}$ (%)	$100 \text{ eV} < E < 1 \text{ keV}$ (%)	$1 \text{ keV} < E < 1 \text{ MeV}$ (%)	$E > 1 \text{ MeV}$ (%)
7	0	18.19	43.81	18.04	18.30	1.66
15	0	19.36	40.70	17.81	20.28	1.85
27	0	20.49	37.63	16.81	22.92	2.15
37	0	21.20	35.47	16.19	24.78	2.36
37	1	12.13	38.79	18.62	27.85	2.61
37	2	8.96	39.24	19.59	29.46	2.76
37	5	5.32	38.72	20.90	32.08	2.99

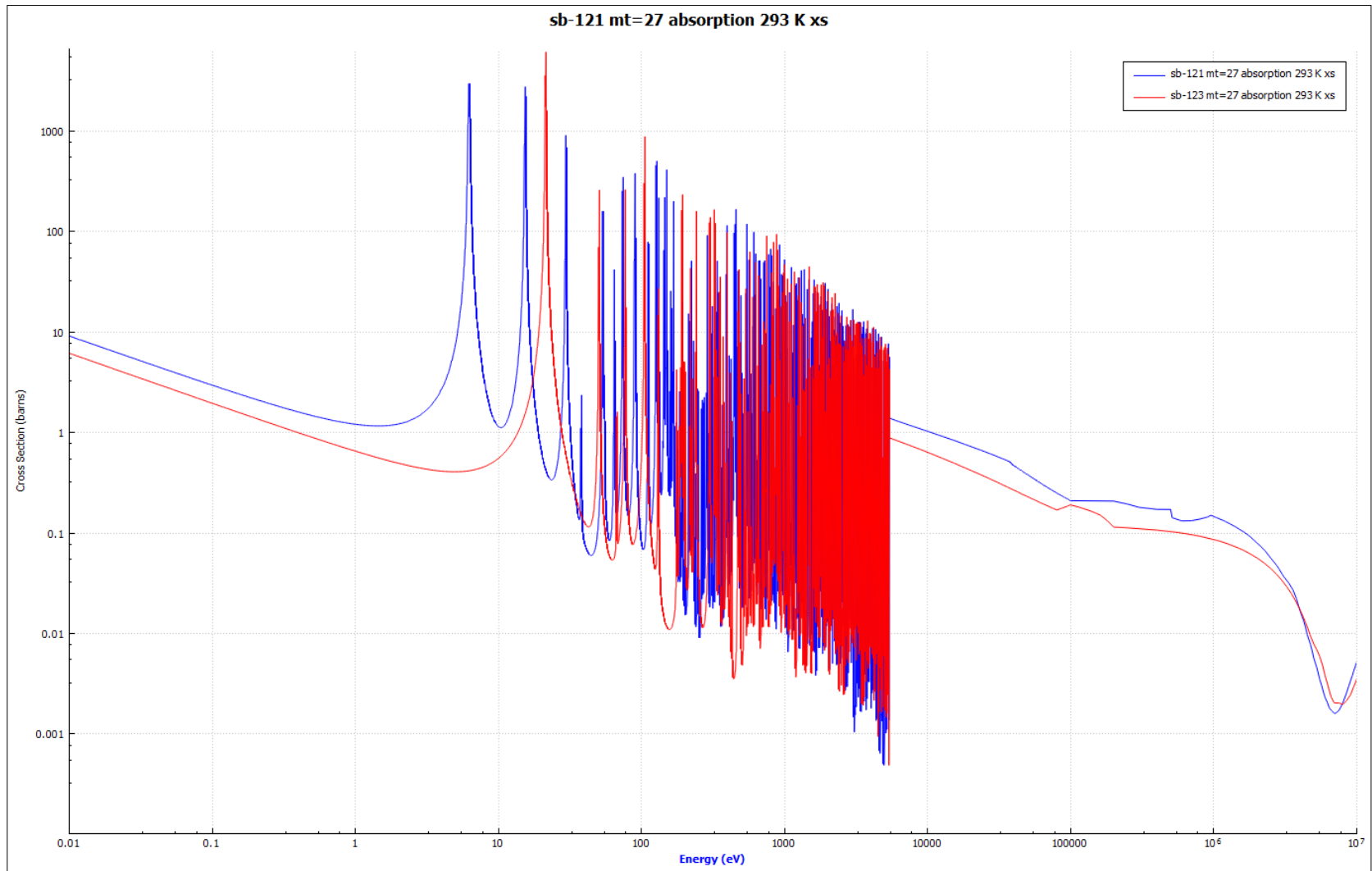


Fig. 28. Energy-dependent absorption cross section for major (>5 wt%) Sb isotopes.

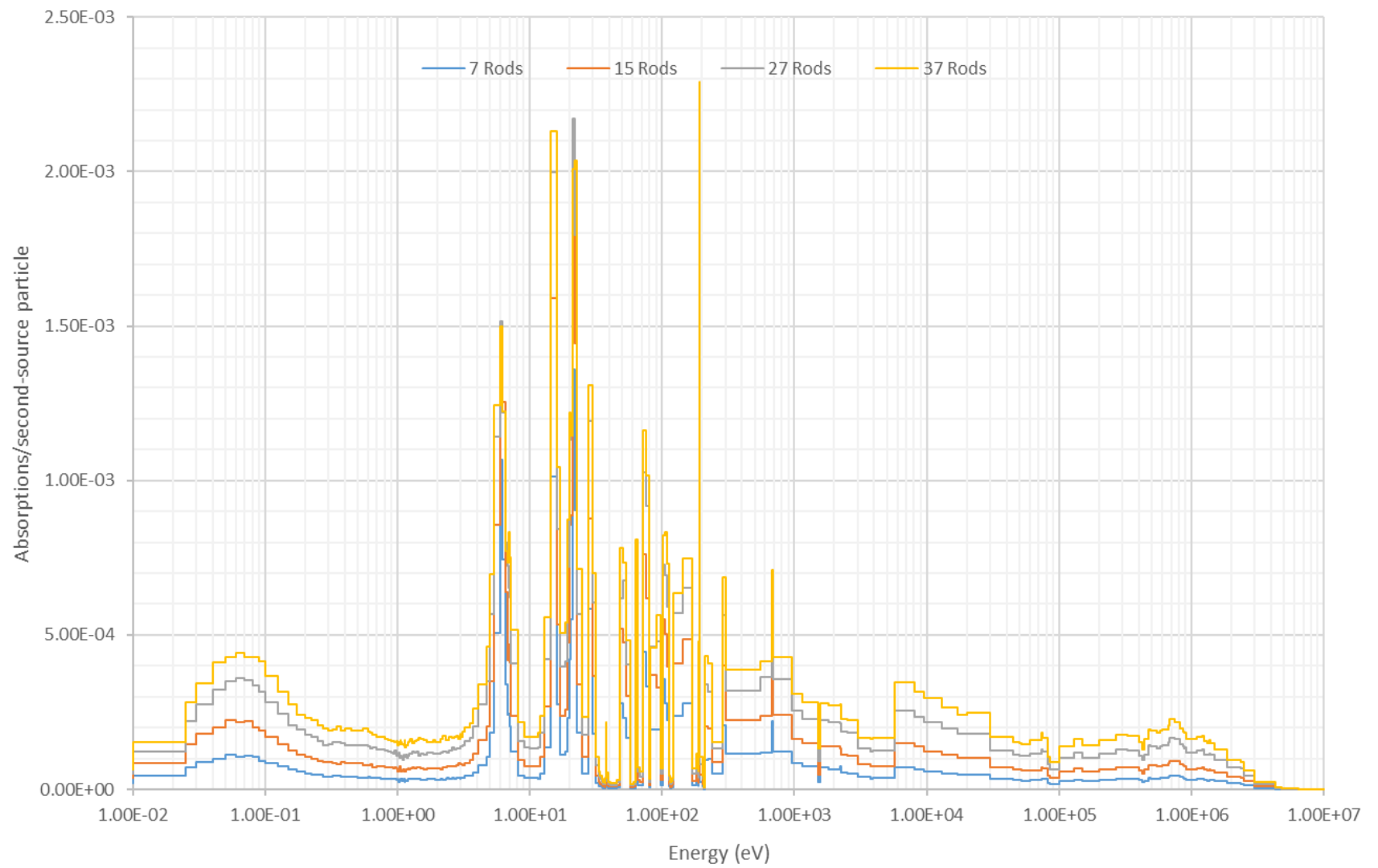


Fig. 29. Energy-dependent reaction rate for a variable number of Sb rods.

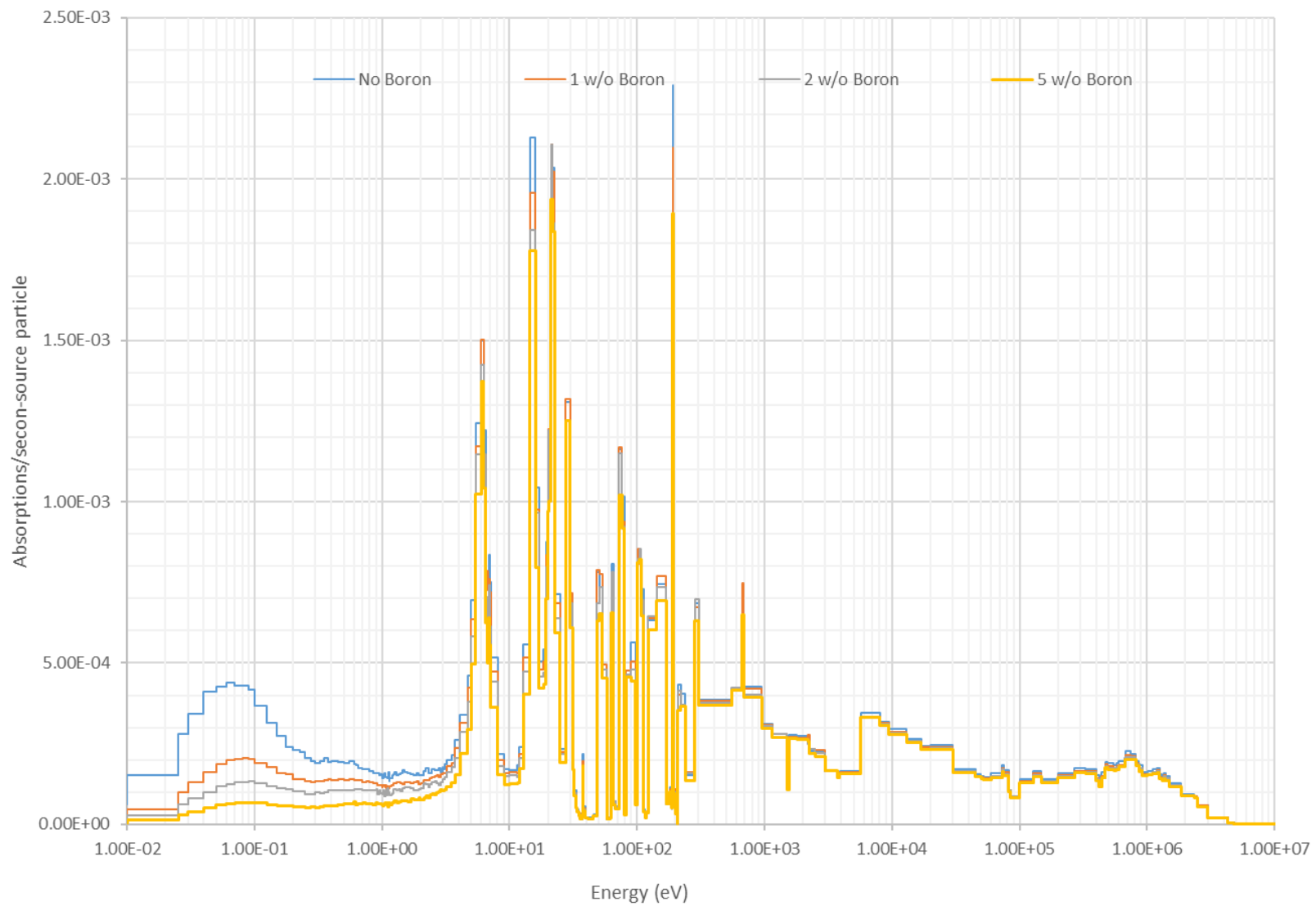


Fig. 30. Energy-dependent reaction rate for ^{37}Sb rods in a central aluminum block with a variable amount of boron.

4. CONCLUSIONS AND CED-2 ACTIONS

This report documents the IER-441 investigation of the ability to test the epithermal/intermediate region of cross sections for various materials. The concept proposed here varies the number of rods and the boron concentration in the central test region of a tight pitched hexagonal lattice with an external driver region to shift the neutron energy spectrum at the location of the test material. Table 12 shows the qualitative results for the potential test materials. Strong absorbers performed well here, and other resonance-based strong absorbers such as Gd and Er would likely make good test materials and should be considered for CED-2 if that data are of interest. At this writing, there is interest in identifying the materials of the greatest interest to the nuclear data community for this project to proceed to CED-2 focused on the clear goal of testing the cross sections of that material.

Table 12. Summary of qualitative assessment of results.

Material	Qualitative result
Dysprosium (Dy)	Good
Indium (In)	Good
Hafnium (Hf)	Good
Silver (Ag)	Good
Tantalum (Ta)	Good
Antimony (Sb)	Moderately good
Cobalt (Co)	Moderately good
Tungsten (W)	Moderately good
Manganese (Mn)	Fair
Vanadium (V)	Poor
Strontium (Sr)	Poor
Molybdenum (Mo)	Poor
Copper (Cu)	Poor
Chromium (Cr)	Poor
Titanium (Ti)	Poor
Niobium (Nb)	Poor
Tin (Sn)	Poor
Iron (Fe)	Poor
Calcium (Ca)	Poor

Table 13 summarizes items to be addressed going forward into CED-2. They are being tracked here to avoid overlooking them as the project progresses. Many of the items can be more easily addressed once one material has been selected.

Table 13. Summary of unresolved comments to be addressed in CED-2

Commenter	Paraphrased comments	Author's notes
MLZ	Tantalum reaction rate looks funny at about 200 eV.	I agree. That is where the resolved resonance region stops and likely where the probability tables take over. This will be further investigated by nuclear data staff at ORNL.
MLZ	Consider possible effects of grain size for the borated aluminum.	This will be examined further when investigation of what is actually procurable is performed in CED-2.
MLZ	Try to develop some configurations with less self-shielding.	I can certainly do that. I can look at not having the test region there and it being flooded. Also can put rods in driver region or close to it.
GAH	Investigate different pin layouts in the test region to see if results can be optimized regarding the pin placement. Look at full rings.	Sounds good for CED-2
GAH	Might be worth lowering boron concentrations for Mn case.	I agree. The boron appears very effective for that case in particular. If that material is desired, then lower boron concentration cases can be analyzed in CED-2
GAH	Consider looking at Gd and Cd instead of B for the material mixed with Al in the test region.	I can look at this in CED-2 easily. Good point.
GAH	Previously mentioned by MLZ: consider diluting samples or using smaller samples to decrease self-shielding in some cases.	I can certainly do that once a material is selected that can be more easily investigated. One of my thoughts is to simply do fuel rod replacement with them to get them in a more thermal spectrum and further apart.
TMM	Not certain I have looked at an exhaustive list of elements.	You are correct. At some point I stopped because I figured I just need to prove the concept now, which I think shows that it works for most strong absorbers. Eventually it gets to be very time consuming to iterate through all of the elements.
TMM	Disagreed with a few of the conclusions for elements.	I think you are right. I tried to provide better definitions for the qualitative rankings. I also incorporated a 5-group energy format to try to be more quantitative.

5. REFERENCES

1. R. M. Westfall et al., *STEM-NEXUS: Safety Technology for Environmental Management – Neutron Spectra Experiments for Underpinning Safety*, ORNL/SPR-2015/567, Oak Ridge National Laboratory, September 30, 2015.
2. G. A. Harms, *Water-Moderated Square-Pitched U(6.90)O₂ Fuel Rod Lattices With 0.67 Fuel to Water Volume Ratio*, LEU-COMP-THERM-080/SAND2014-2156P, Sandia National Laboratories, September 2013.
3. G. A. Harms, *Partially-Reflected Water-Moderator Square-Pitched U(6.90)O₂ Fuel Rod Lattices with 0.67 Fuel to Water Volume Ratio (0.800 cm Pitch)*, LEU-COMP-THERM-096/SAND2015-7734 R, Sandia National Laboratories, September 2015.
4. G. A. Harms, *Titanium and/or Aluminum Rod-Replacement Experiments in Fully-Reflected Water-Moderated Square-Pitched U(6.90)O₂ Lattices with a 0.67 Fuel to Water Volume Ratio (0.800 cm Pitch)*, LEU-COMP-THERM-097/SAND2016-9686 R, Sandia National Laboratories, September 2016.
5. *3MTM 10B Enriched Borated Aluminum*, 3M Ceradyne Canada, ULC, Chicoutimi, Quebec, Canada, July 2015.